The simulation predicts everything – it is consistent with every outcome anticipated

"The Nature of Scientific Proof in the Age of Simulations"

Kevin Heng

Dissipation @ light cylinder

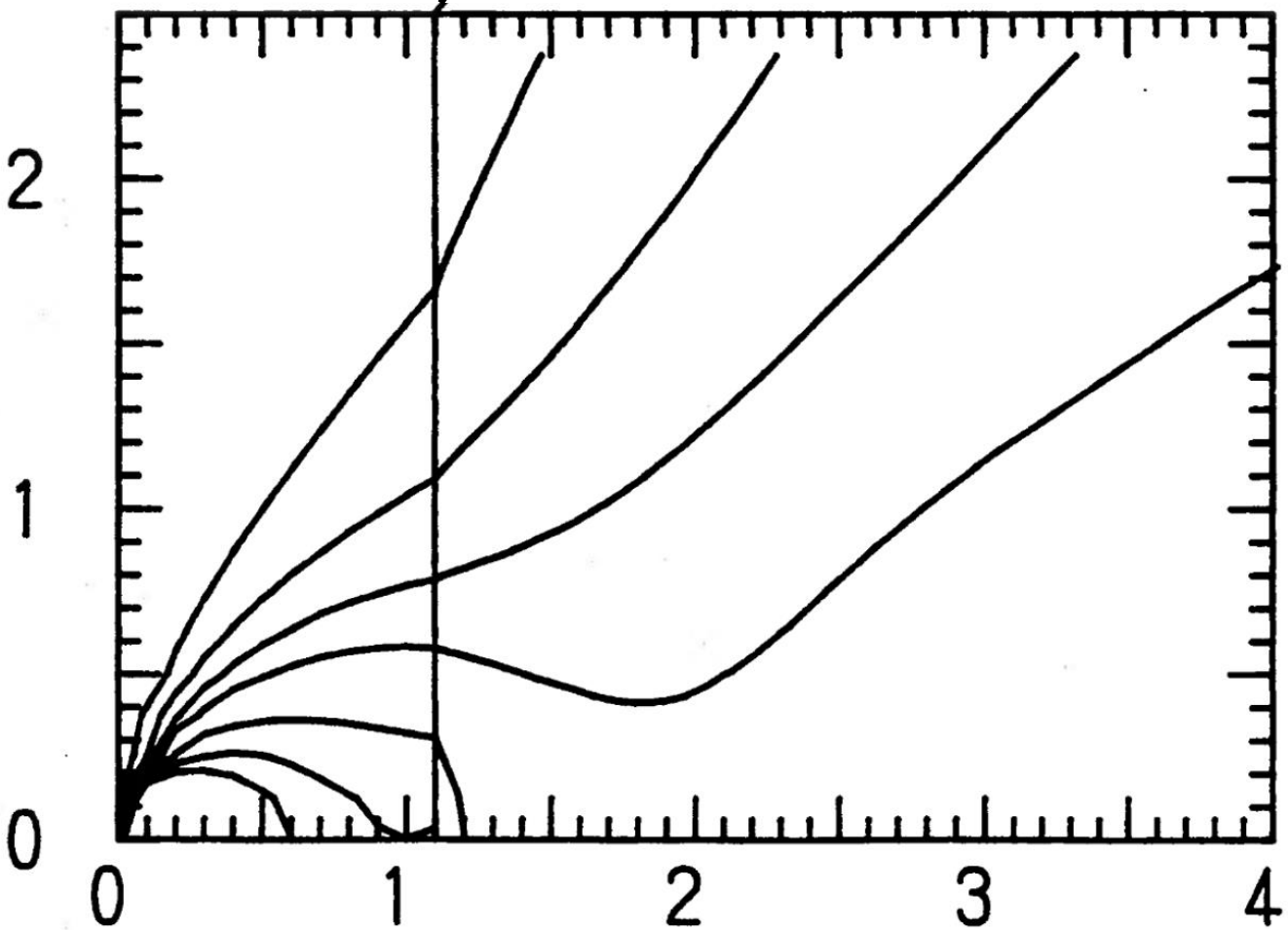

"The axisymmetric pulsar magnetosphere: a new model", Mestel & Shibata 1994

No dissipation @ light cylinder

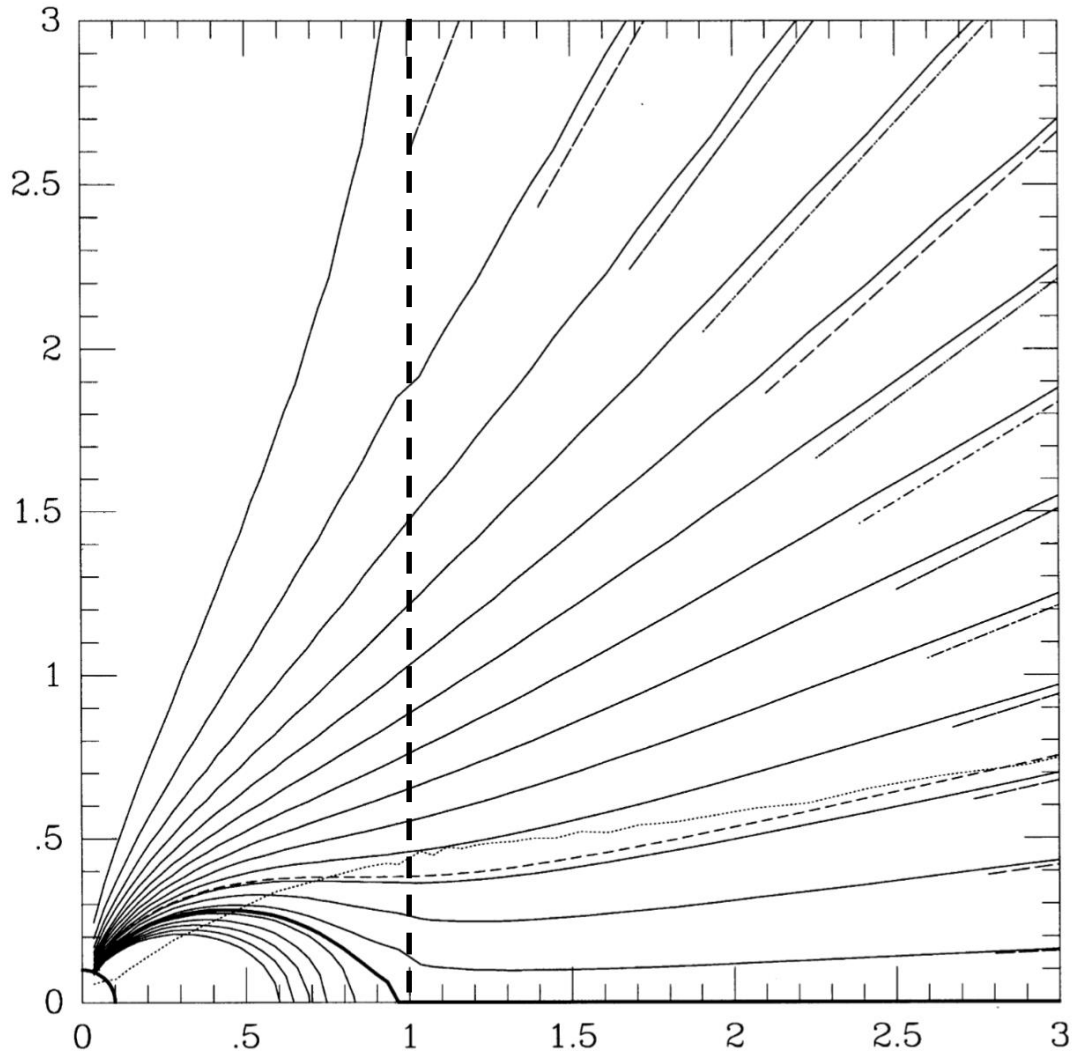

"The axisymmetric pulsar magnetosphere", Contopoulos, Kazanas & Fendt 1999

No dissipation @ current sheet

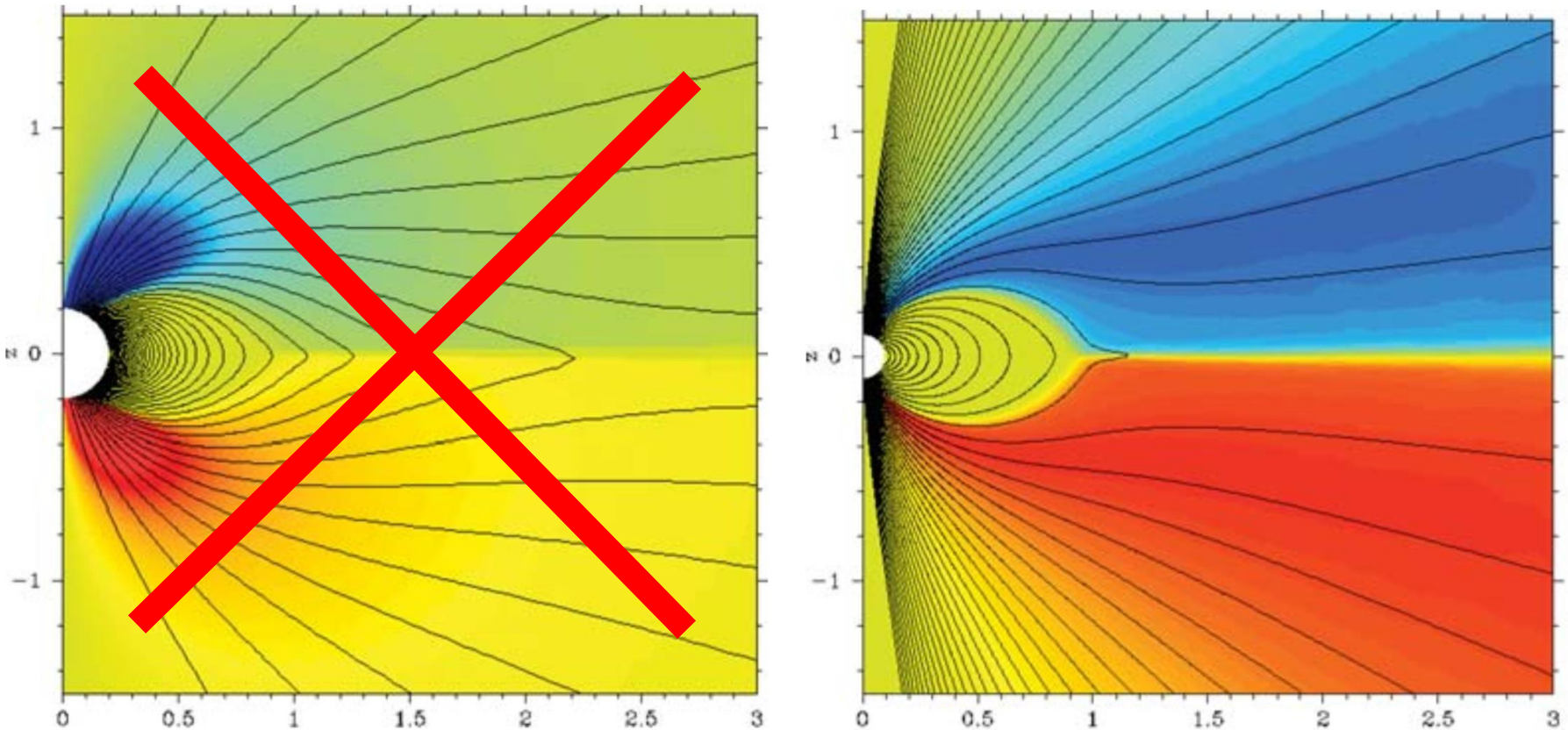

"Simulations of the axisymmetric magnetospheres of neutron stars", Komissarov 2006

No dissipation @ current sheet

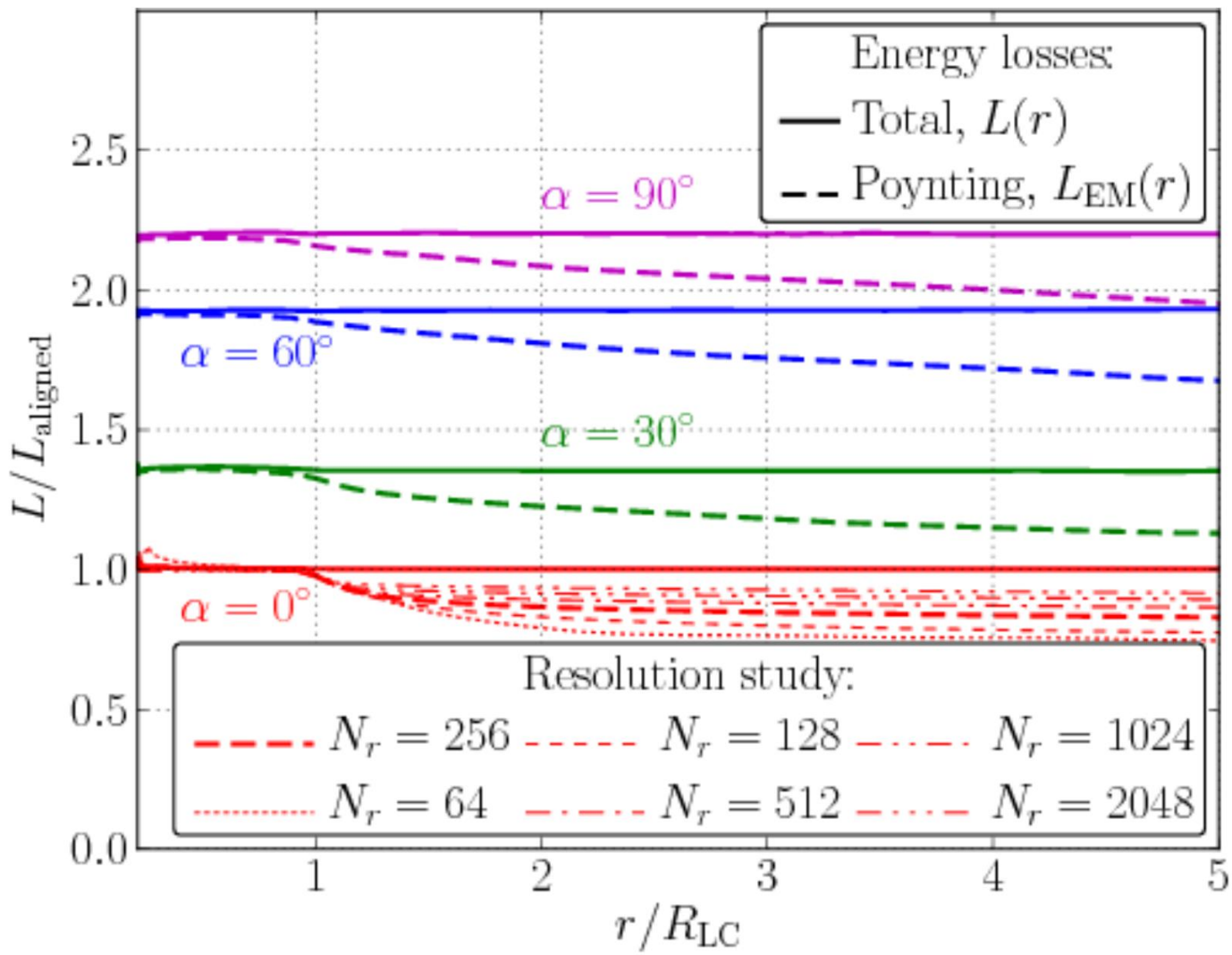

"Ab initio pulsar magnetospheres", Philippov & Spitkovsky 2014

No dissipation @ current sheet

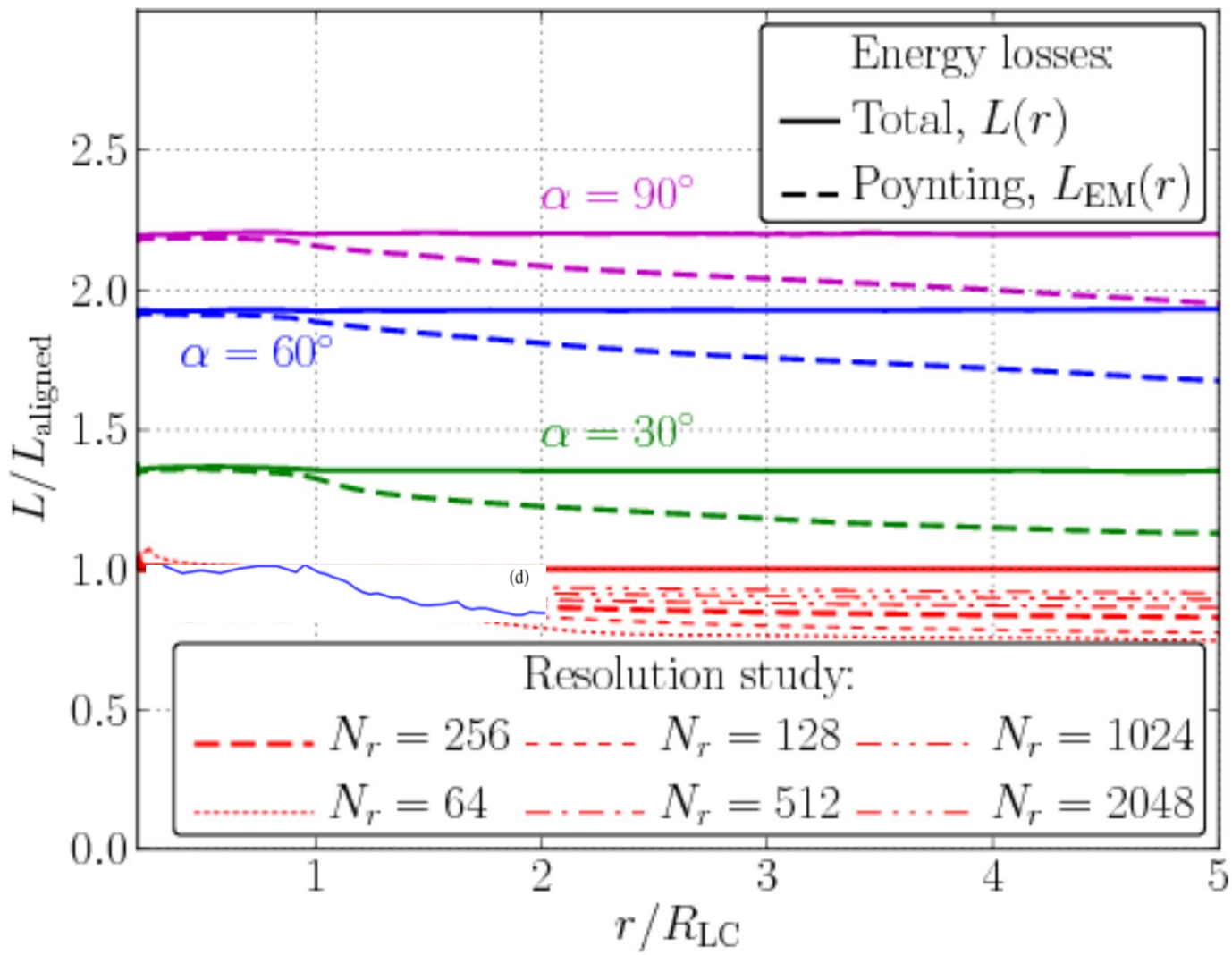

"Ab initio pulsar magnetospheres", Philippov & Spitkovsky 2014

High-energy radiation → Dissipation

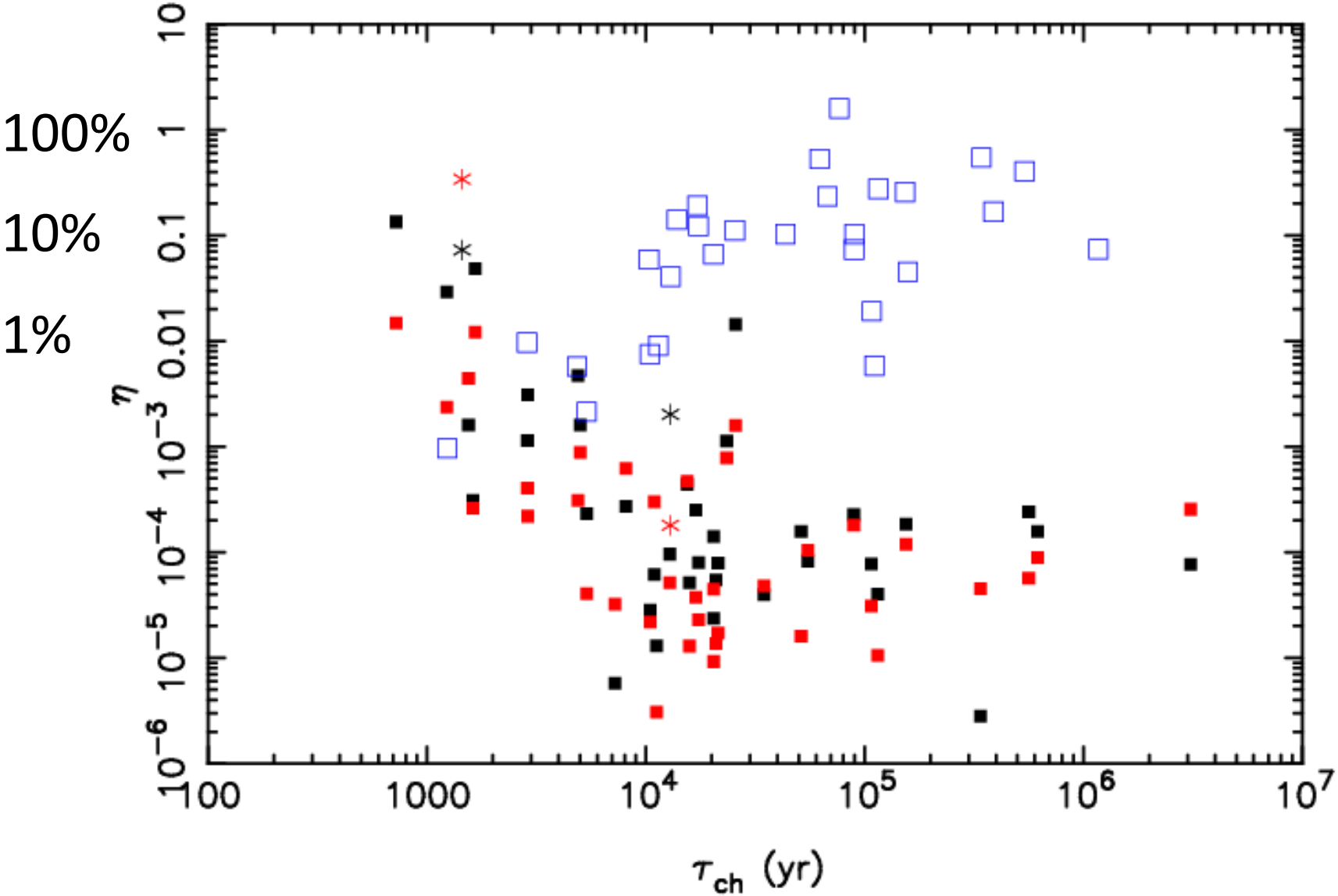

Dissipation @ current sheet

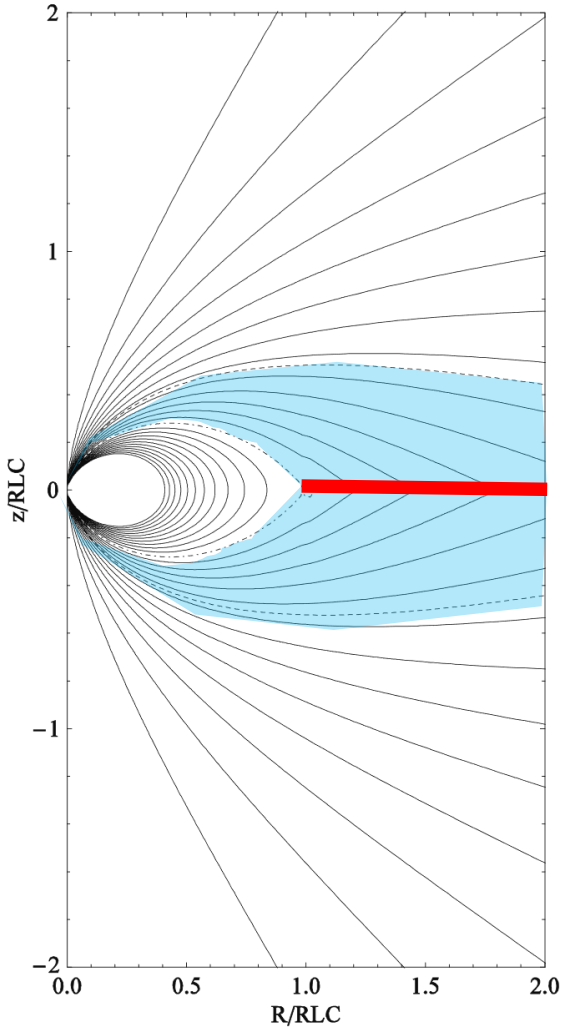

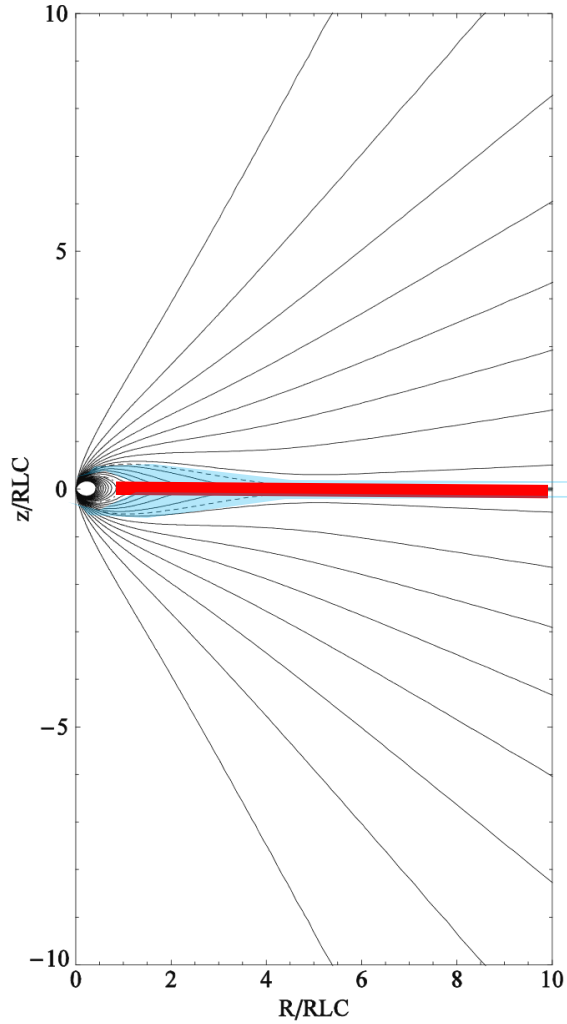

"A new standard pulsar magnetosphere", Contopoulos 2014

"The role of reconnection in the pulsar magnetosphere", Contopoulos 2007

Dissipation @ current sheet

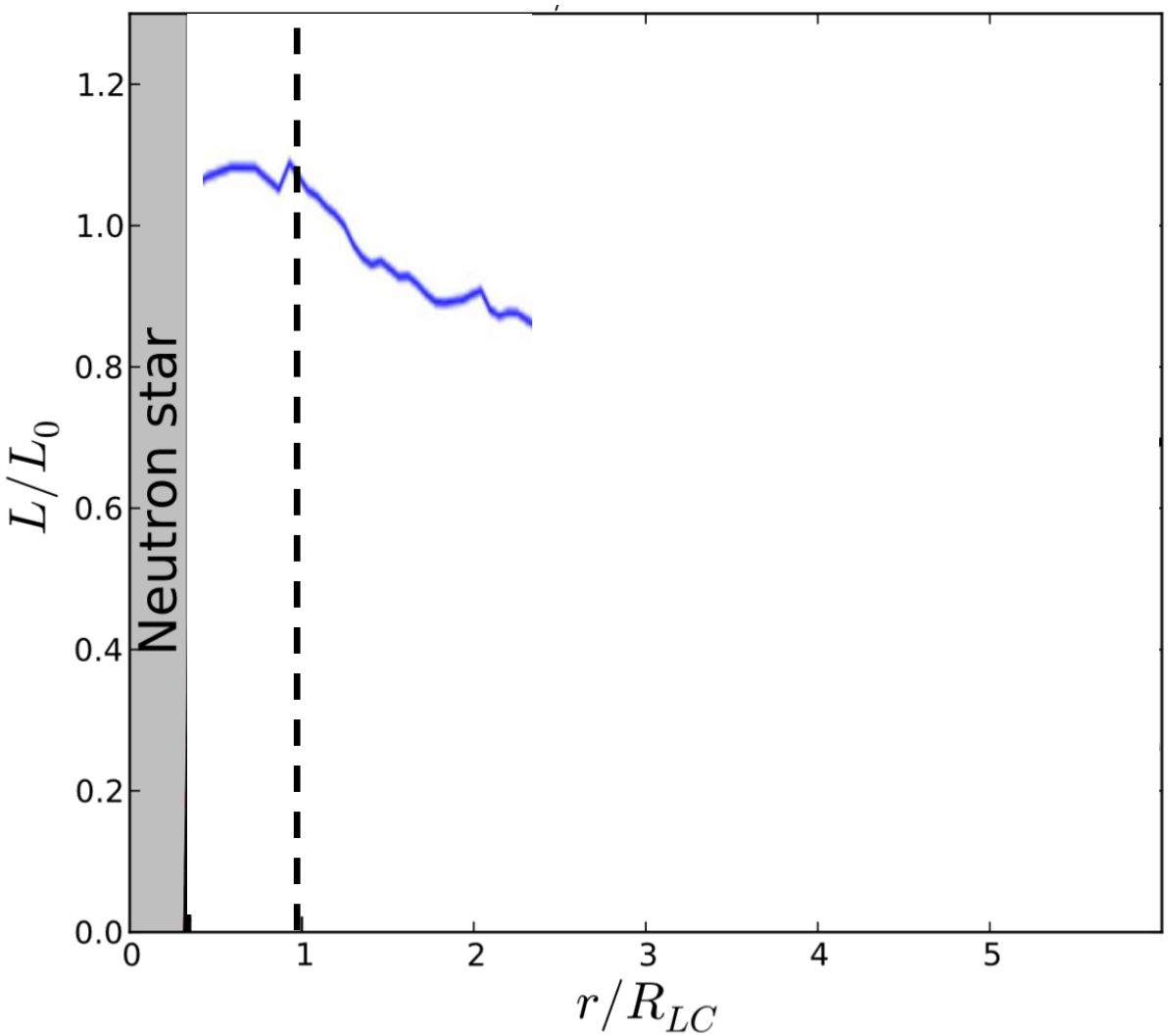

"Ab initio pulsar magnetospheres", Philippov & Spitkovsky 2014

Dissipation @ current sheet

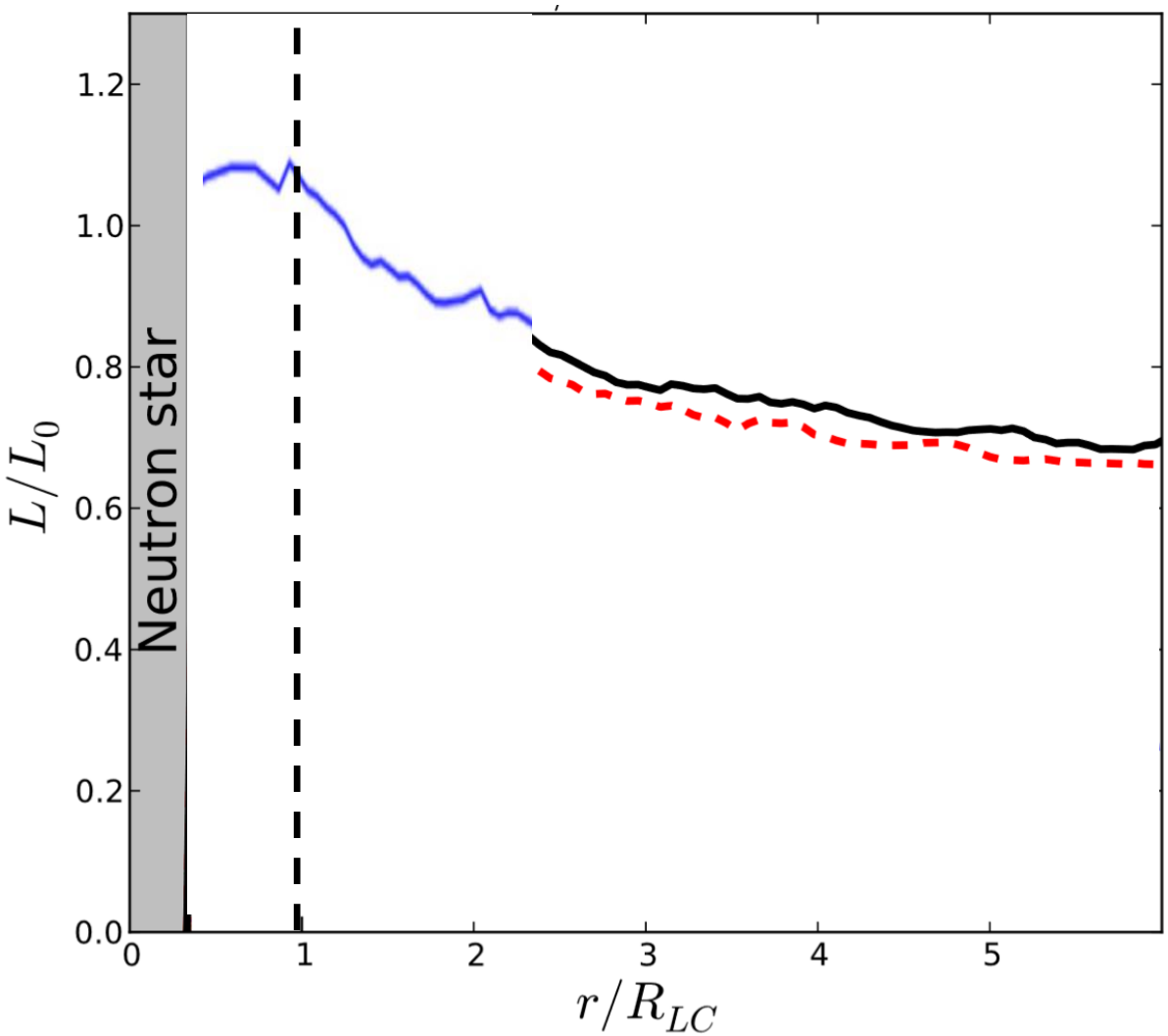

"Particle acceleration in pulsar current sheets", Cerutti, Philippov, Parfrey & Spitkovsky 2015

Κέντρο Ερευνών Αστρονομίας
και Εφαρμοσμένων Μαθηματικών
της Ακαδημίας Αθηνών

A ”ring of fire” in the pulsar magnetosphere

Ioannis Contopoulos

Research Center for Astronomy, Academy of Athens

NASA/Goddard, June 10, 2019

Collaborators: Petros Stefanou (Athens), Jérôme Pétri (Strasbourg)

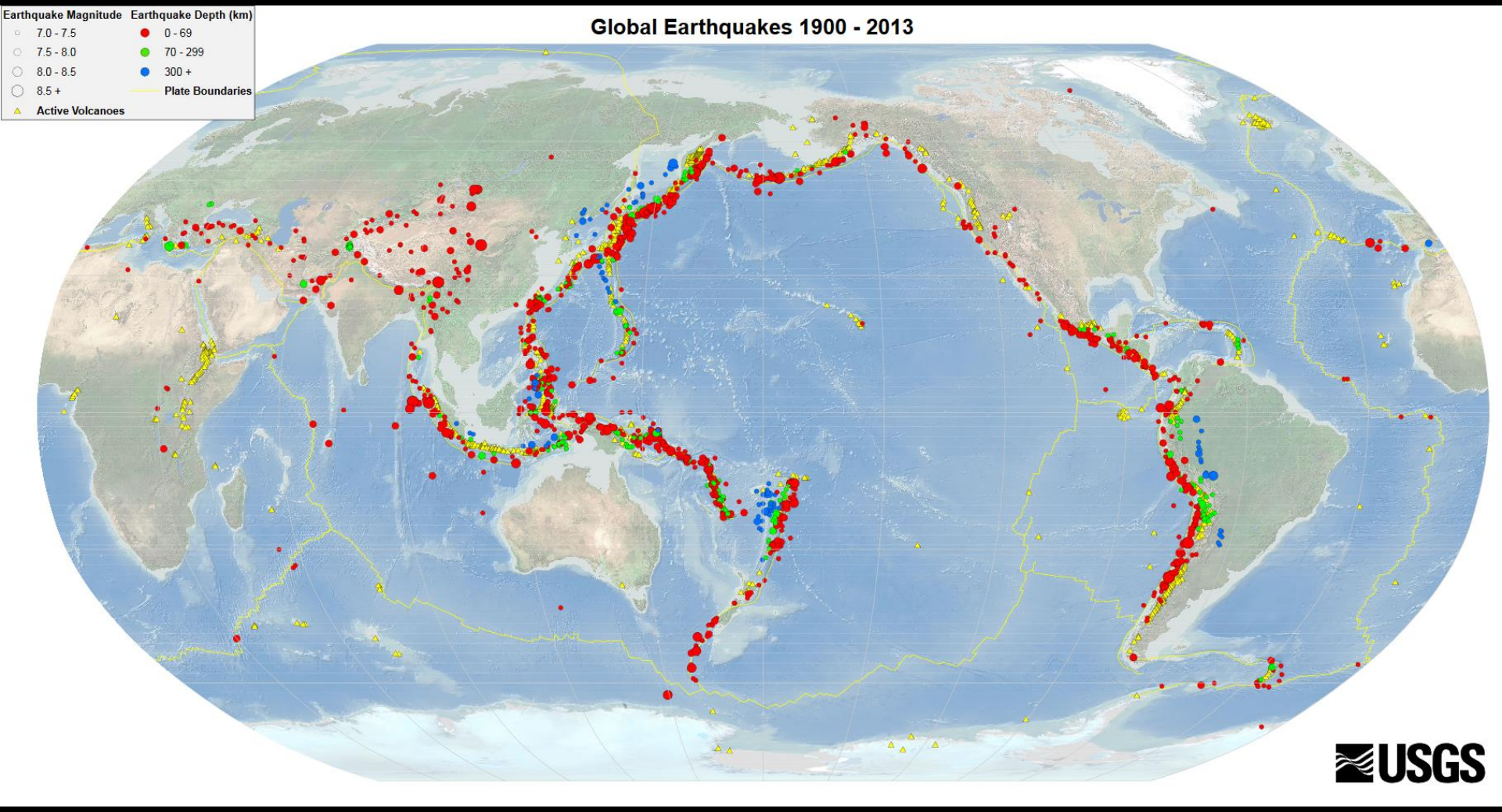
Global Earthquakes 1900 - 2013
Earthquake Magnitude
7.0 - 7.5
7.5 - 8.0
8.0 - 8.5
8.5 +
Active Volcanoes
Earthquake Depth (km)
0 - 69
70 - 299
300 +
Plate Boundaries
USGS

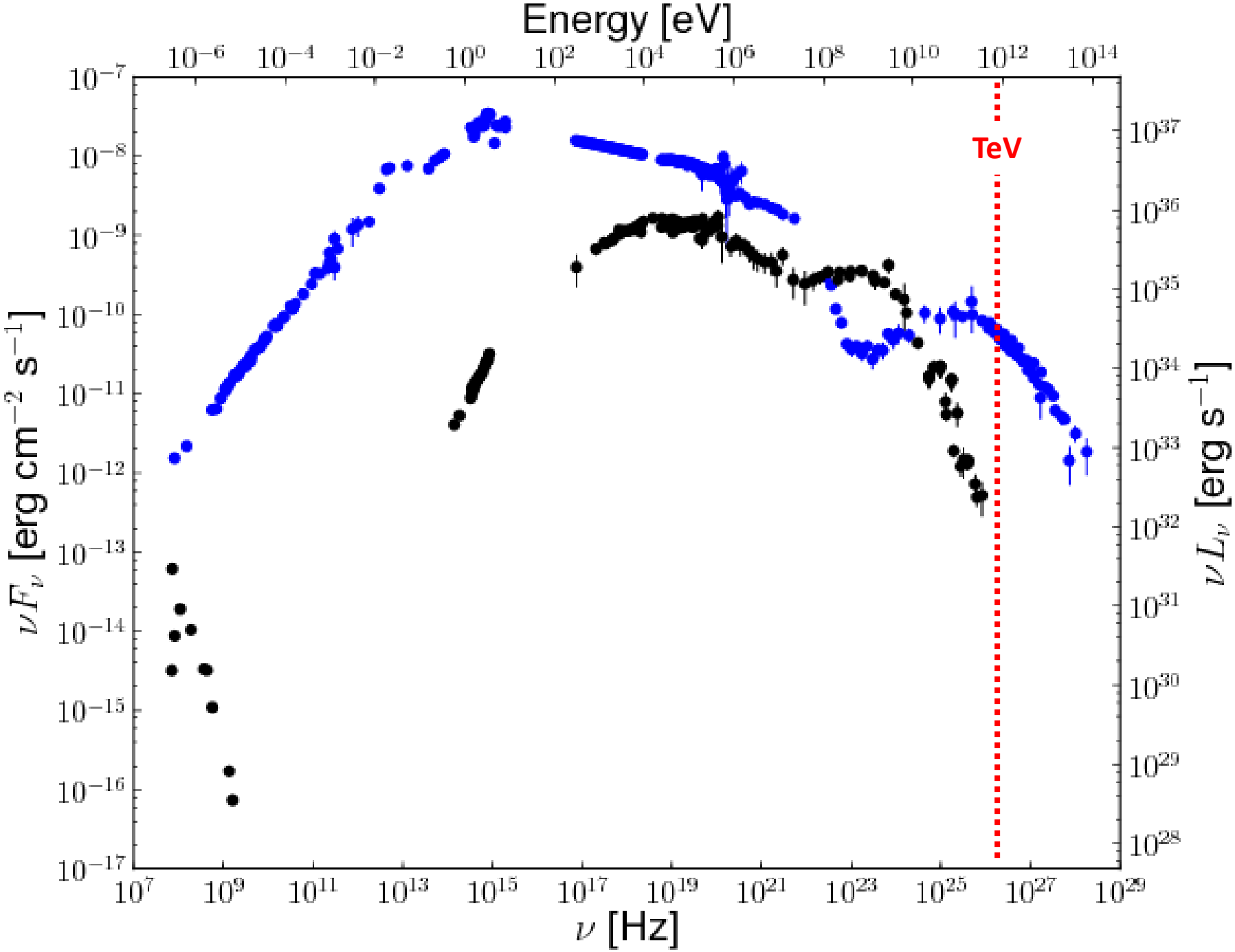
Energy [eV]
10^{-6} 10^{-4} 10^{-2} 10^{0} 10^{2} 10^{4} 10^{6} 10^{8} 10^{10} 10^{12} 10^{14}
TeV
νF_ν [erg cm^{-2} s^{-1}]
10^{-7} 10^{-8} 10^{-9} 10^{-10} 10^{-11} 10^{-12} 10^{-13} 10^{-14} 10^{-15} 10^{-16} 10^{-17}
νL_ν [erg s^{-1}]
10^{37} 10^{36} 10^{35} 10^{34} 10^{33} 10^{32} 10^{31} 10^{30} 10^{29} 10^{28}
ν [Hz]
10^{7} 10^{9} 10^{11} 10^{13} 10^{15} 10^{17} 10^{19} 10^{21} 10^{23} 10^{25} 10^{27} 10^{29}

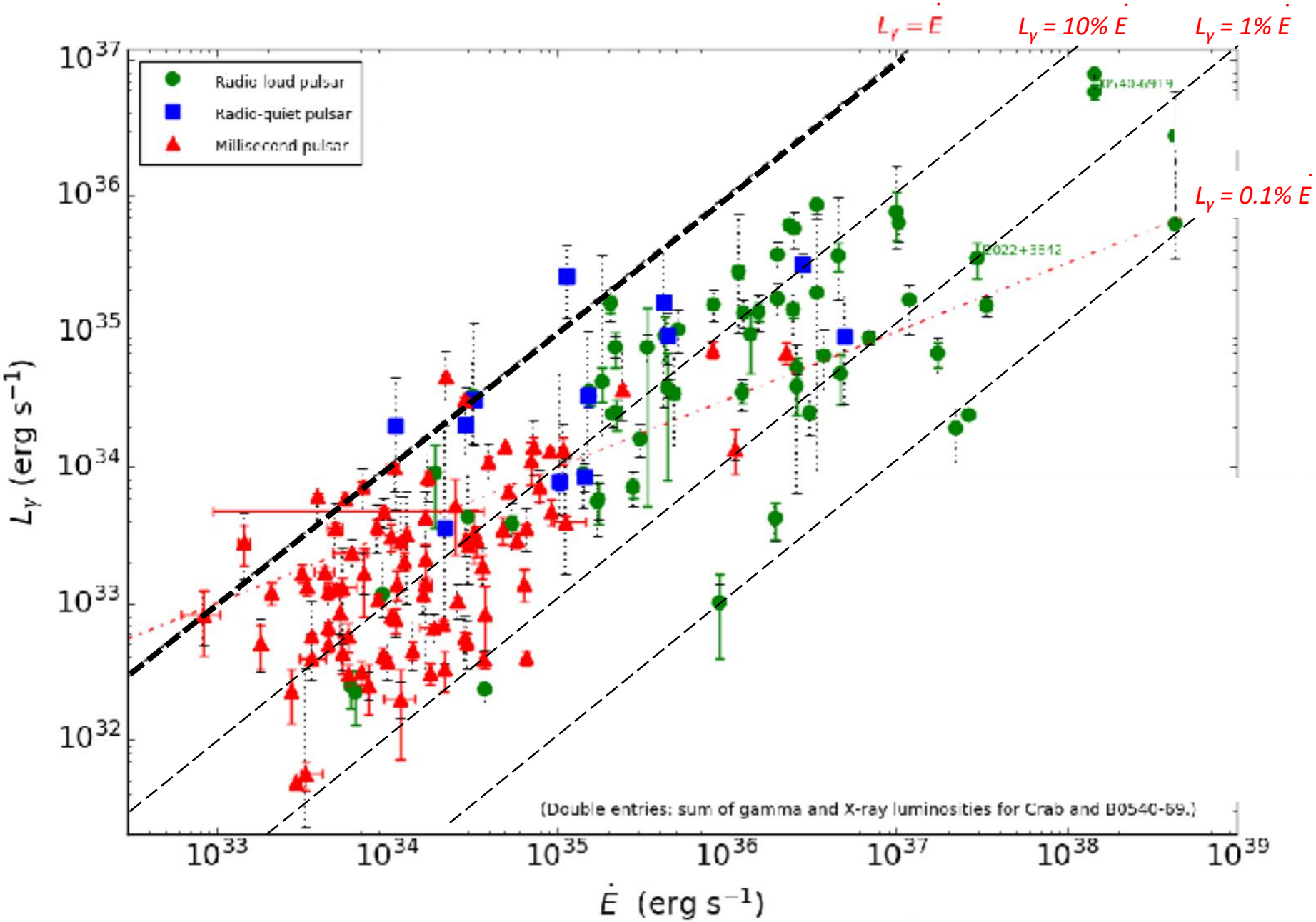
$L_\gamma = \dot{E}$
$L_\gamma = 10\% \dot{E}$
$L_\gamma = 1\% \dot{E}$
$L_\gamma = 0.1\% \dot{E}$
Radio loud pulsar
Radio-quiet pulsar
Millisecond pulsar
(Double entries: sum of gamma and X-ray luminosities for Crab and B0540-69.)
L_γ (erg s^{-1})
$\dot{E}$ (erg s^{-1})
10^{32}
10^{33}
10^{34}
10^{35}
10^{36}
10^{37}
10^{38}
10^{39}

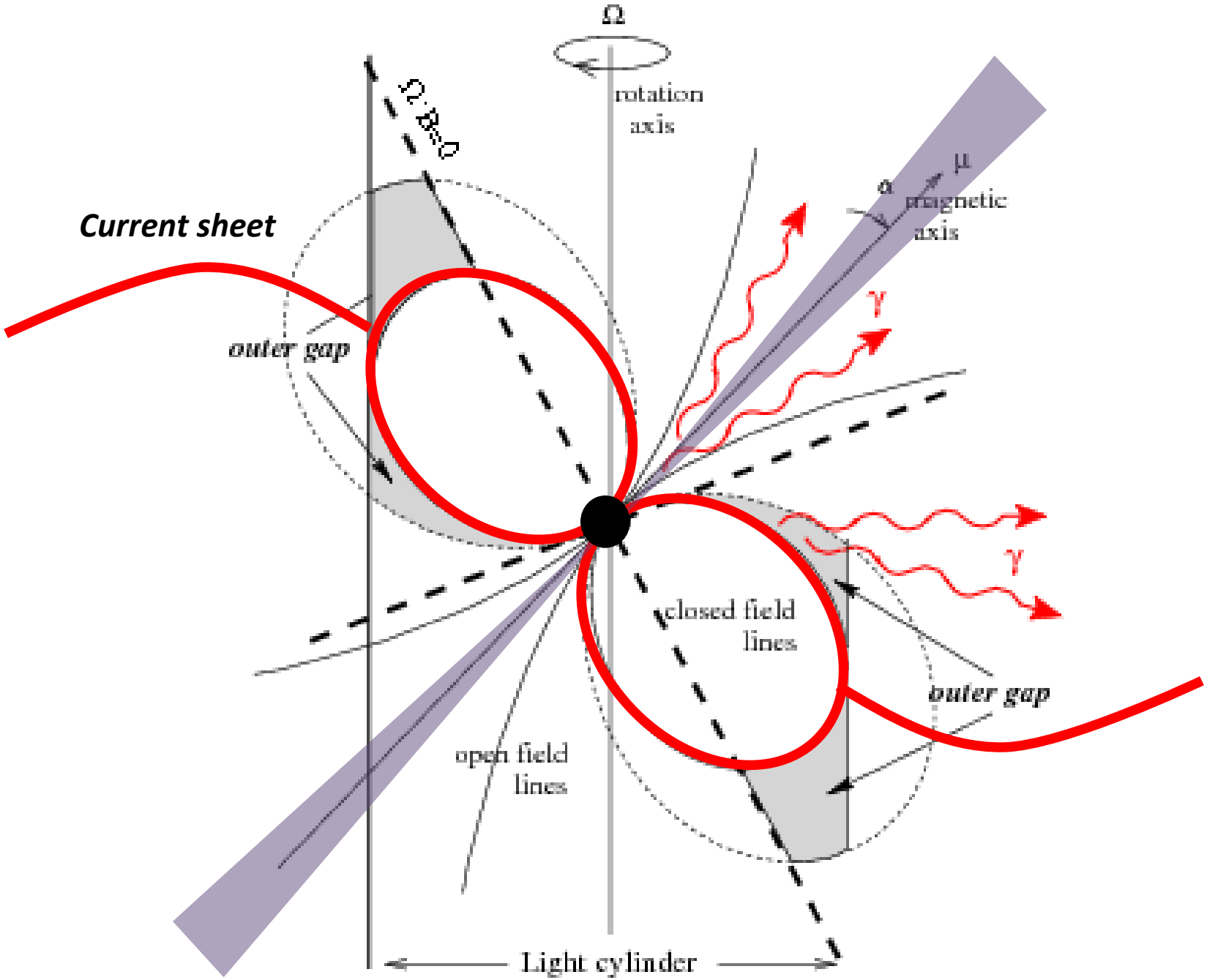
Current sheet
Ω
rotation
axis
μ
α
magnetic
axis
γ
γ
outer gap
outer gap
closed field
lines
open field
lines
Light cylinder

Non-ideal magnetospheres (non-ideal prescriptions…)

2012 (Spitkovsky et al.)
2012 (Contopoulos, Kalapotharakos et al.)

2. NON-IDEAL PRESCRIPTIONS

In the FFE description of pulsar magnetospheres, Spitkovsky (2006) and Kalapotharakos & Contopoulos (2009) solved numerically the time-dependent Maxwell equations

$$\frac{\partial \mathbf{B}}{\partial t} = -c\nabla \times \mathbf{E} \tag{1}$$

$$\frac{\partial \mathbf{E}}{\partial t} = c\nabla \times \mathbf{B} - 4\pi \mathbf{J} \tag{2}$$

under ideal force-free conditions

$$\mathbf{E} \cdot \mathbf{B} = 0, \quad \rho \mathbf{E} + \frac{1}{\mathbf{c}} \mathbf{J} \times \mathbf{B} = 0,$$

where $\rho = \nabla \cdot \mathbf{E}/(4\pi)$. The evolution of these equations in time requires in addition an expression for the current density $\mathbf{J}$ as a function of $\mathbf{E}$ and $\mathbf{B}$. This is given by

$$\mathbf{J} = c\rho \frac{\mathbf{E} \times \mathbf{B}}{B^2} + \frac{c}{4\pi} \frac{\mathbf{B} \cdot \nabla \times \mathbf{B} - \mathbf{E} \cdot \nabla \times \mathbf{E}}{B^2} \mathbf{B} \tag{3}$$

(A) The above implementation of the ideal condition hints at an easy generalization that leads to non-ideal solutions: one can evolve Equations (1) and (2), using only the first term of the FFE current density (Equation (3)), and at each time step keep only a certain fraction b of the $\mathbf{E}_{||}$ developed during this time instead of forcing it to be zero. In general, the portion b of the remaining $\mathbf{E}_{||}$ can be either the same everywhere or variable (locally) depending on some other quantity (e.g., ρ, J). As b goes from 0 to 1, the corresponding solution goes from FFE to vacuum. In this case, an expression for the electric current density is not given a priori, and $\mathbf{J}$ can be obtained indirectly from the expression

$$\mathbf{J} = \frac{1}{4\pi} \left(c\nabla \times \mathbf{B} - \frac{\partial \mathbf{E}}{\partial t} \right). \tag{4}$$

(B) Another way of controlling $\mathbf{E}_{||}$ is to introduce a finite conductivity σ. In this case, we replace the second term in Equation (3) by $\sigma \mathbf{E}_{||}$ and the current density reads

$$\mathbf{J} = c\rho \frac{\mathbf{E} \times \mathbf{B}}{B^2} + \sigma \mathbf{E}_{||}. \tag{5}$$

Note that Equation (5) is related to but is not quite equivalent to Ohm's law, which is defined in the frame of the fluid. Others

non-dissipative. The current density expression in the so-called strong field electrodynamics (hereafter SFE) reads

$$\mathbf{J} = \frac{c\rho \mathbf{E} \times \mathbf{B} + (c^2\rho^2 + \gamma^2\sigma^2 E_0^2)^{1/2}(B_0 \mathbf{B} + E_0 \mathbf{E})}{B^2 + E_0^2}, \tag{6}$$

where

$$B_0^2 - E_0^2 = \mathbf{B}^2 - \mathbf{E}^2, \quad B_0 E_0 = \mathbf{E} \cdot \mathbf{B}, \quad E_0 \geqslant 0, \tag{7}$$

$$\gamma^2 = \frac{B^2 + E_0^2}{B_0^2 + E_0^2}, \tag{8}$$

Radiation from particle trajectories with β=1…

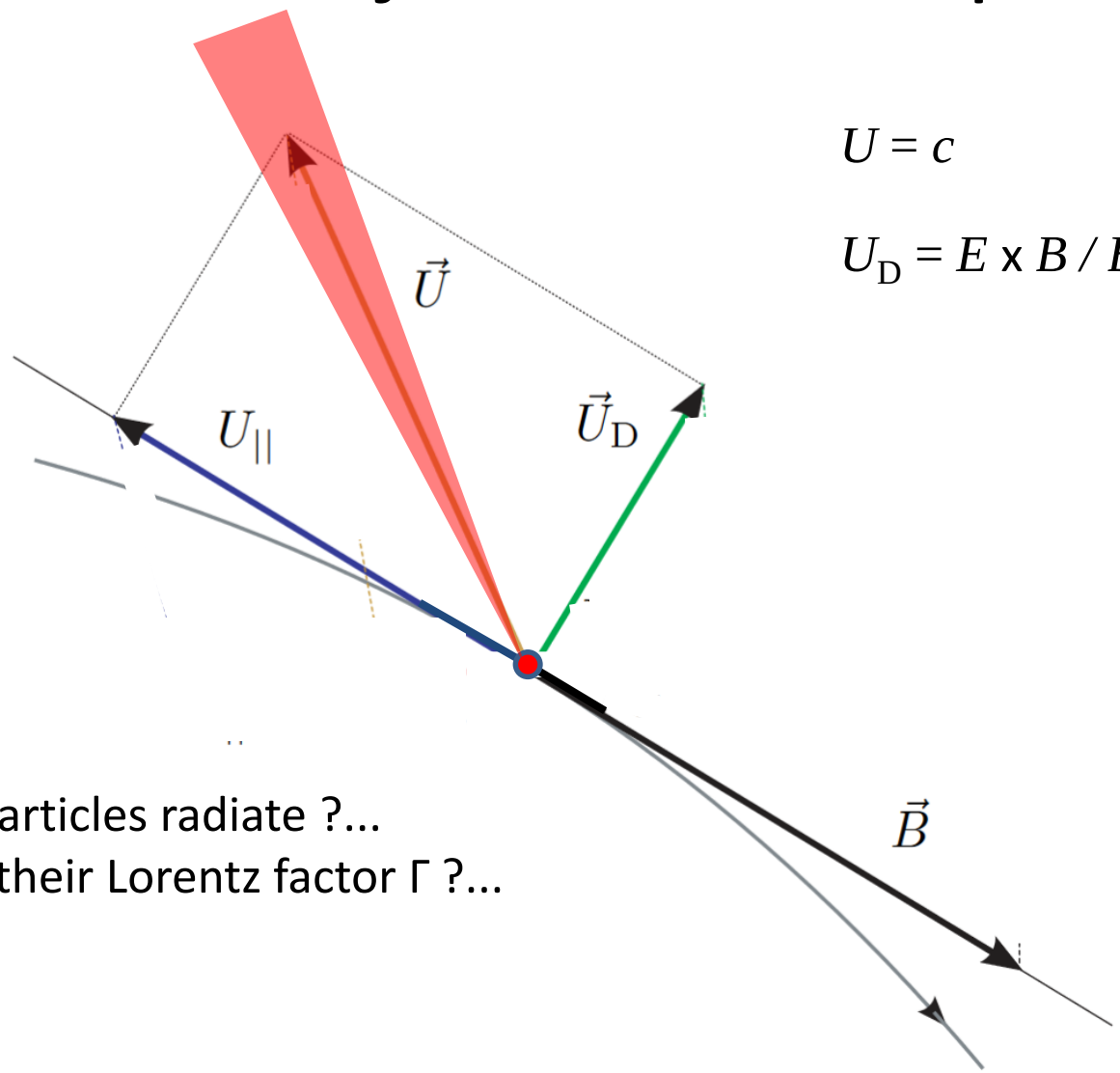

$U = c$

$U_{\mathrm{D}} = E \times B / B^2$

Which particles radiate ?...
What is their Lorentz factor Γ ?...

3D “ab initio” Particle-in-Cell

2014 (Spitkovsky + Sironi, Cerutti et al.)
2016 (Kalapotharakos)

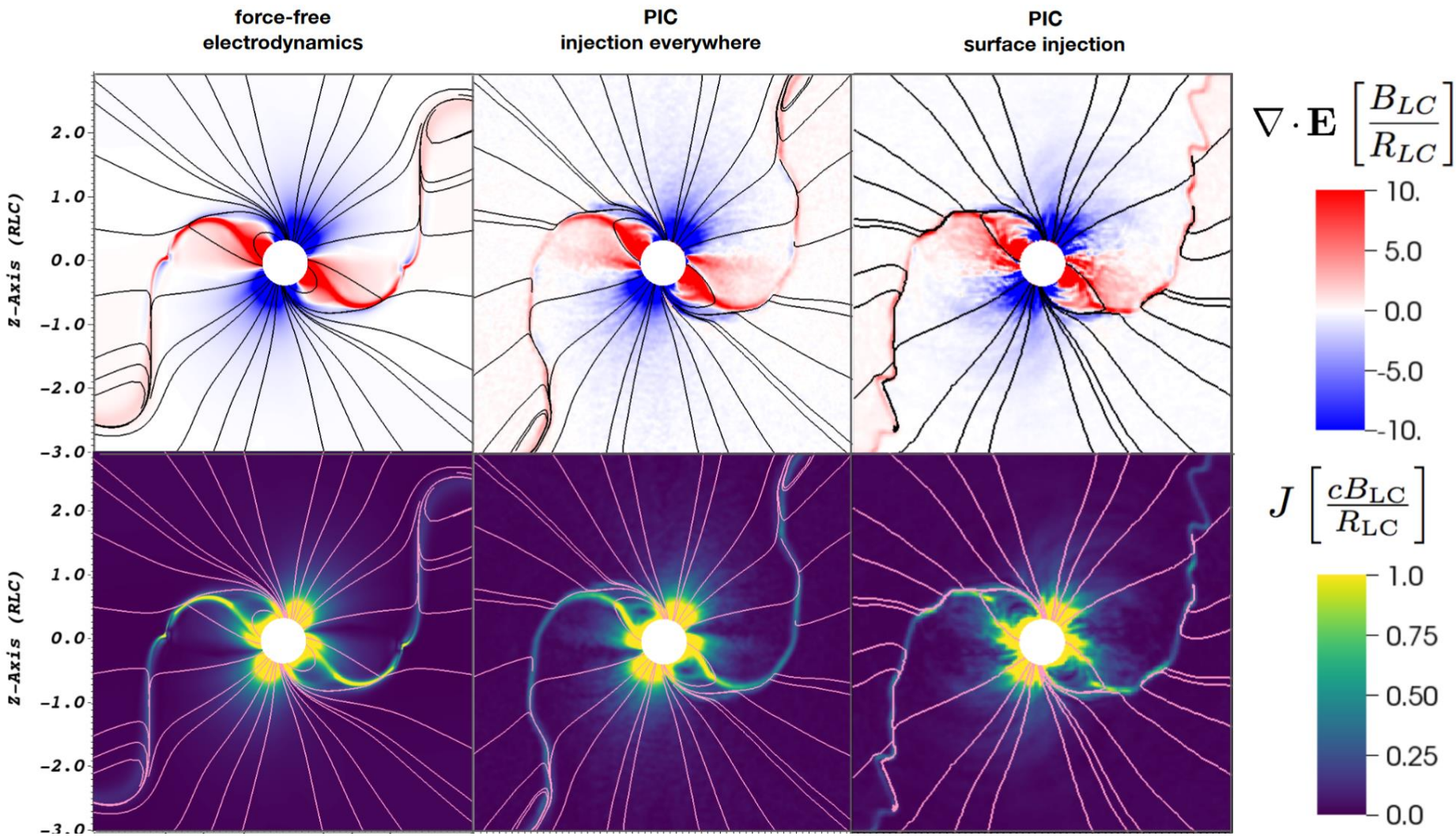

Brambilla, Kalapotharakos et al. 2018

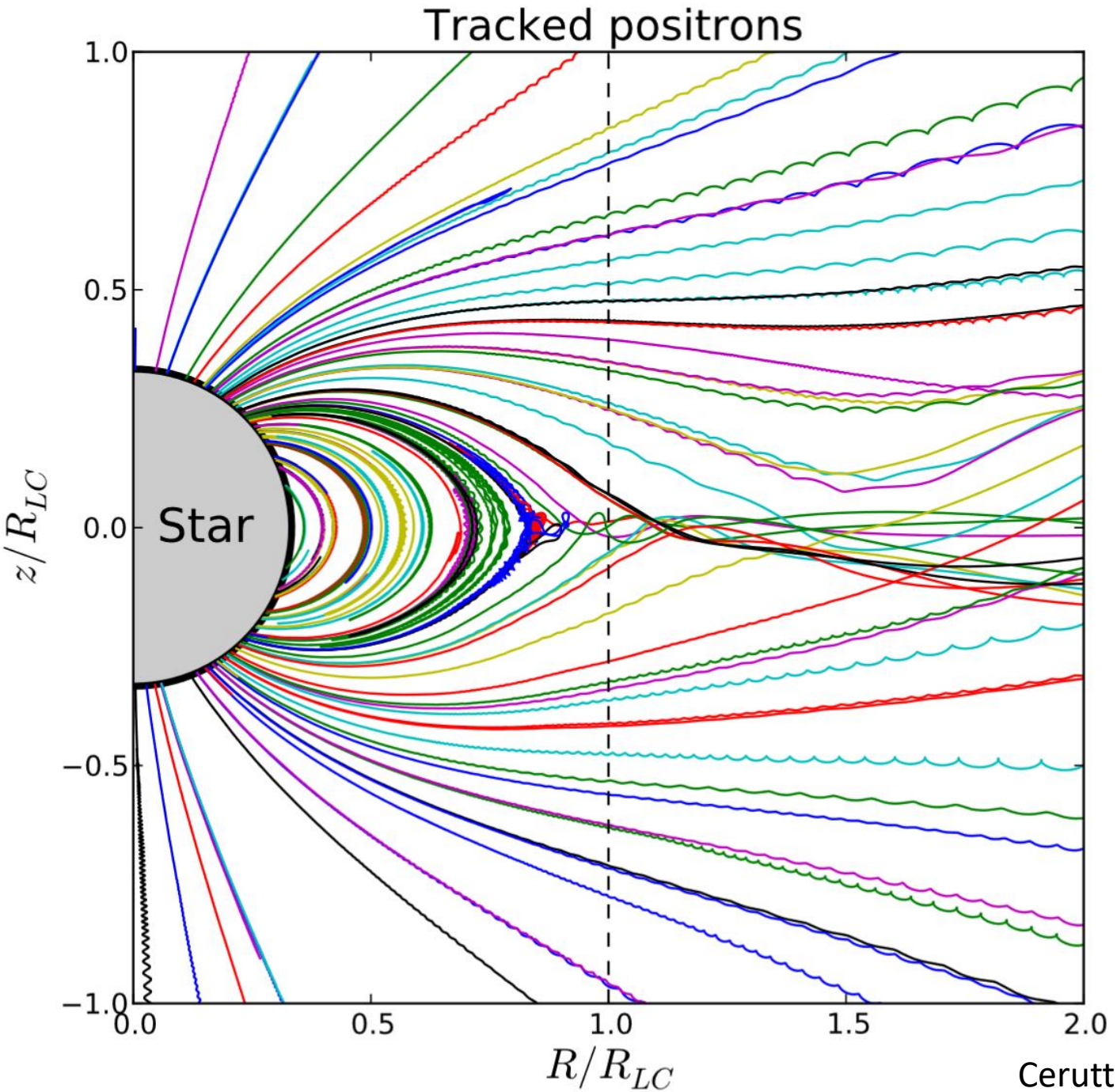

Cerutti et al. 2015

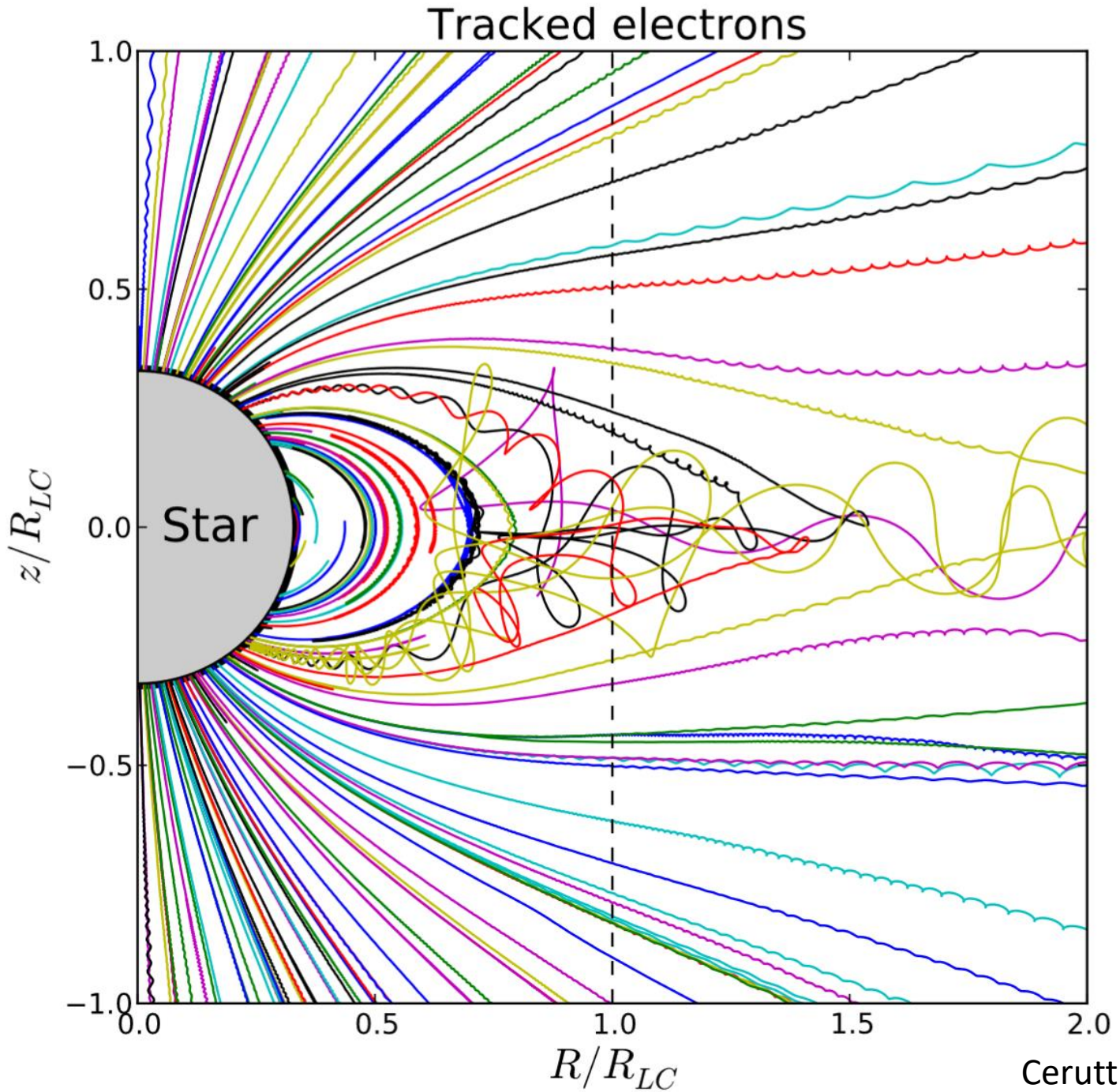

Cerutti et al. 2015

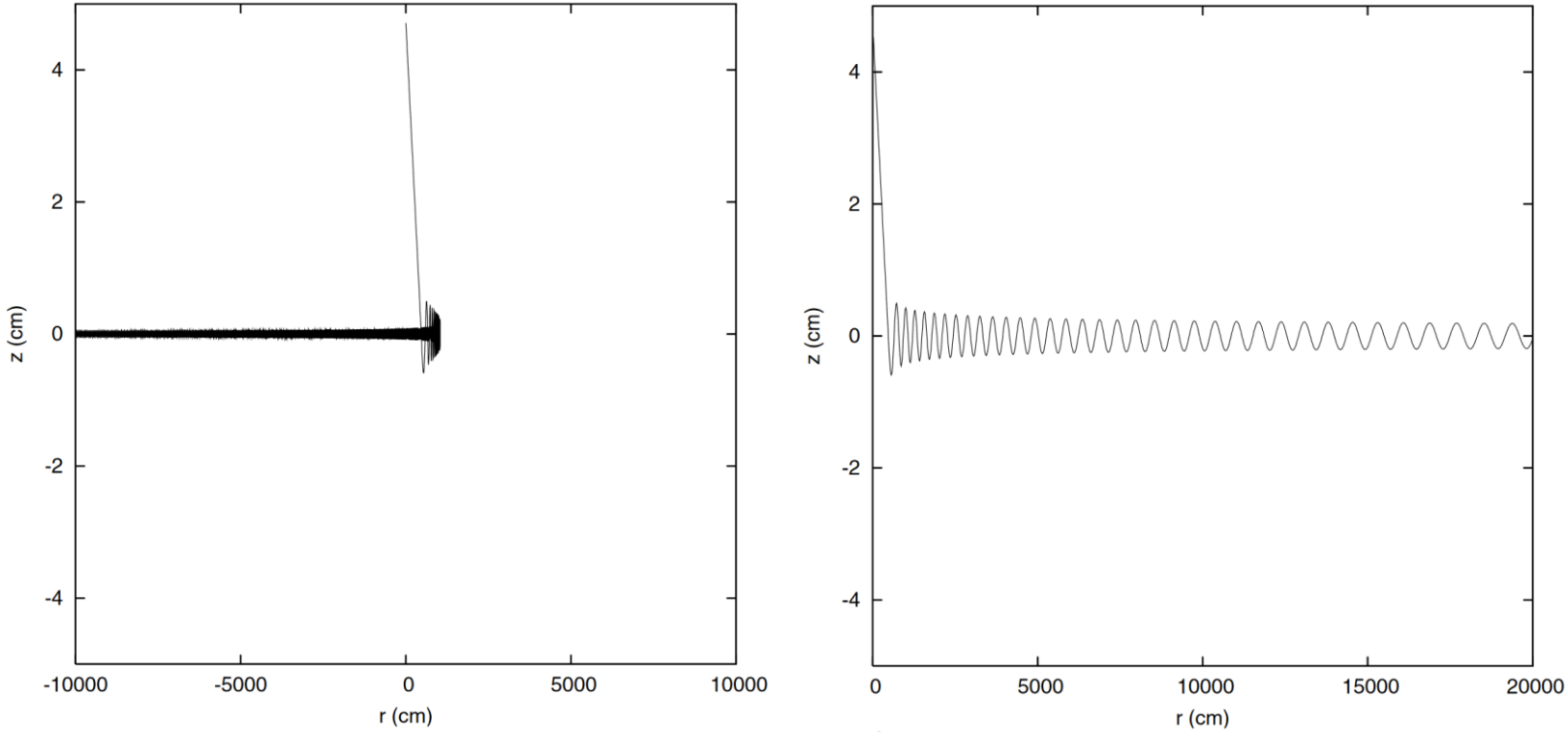

Speiser orbits

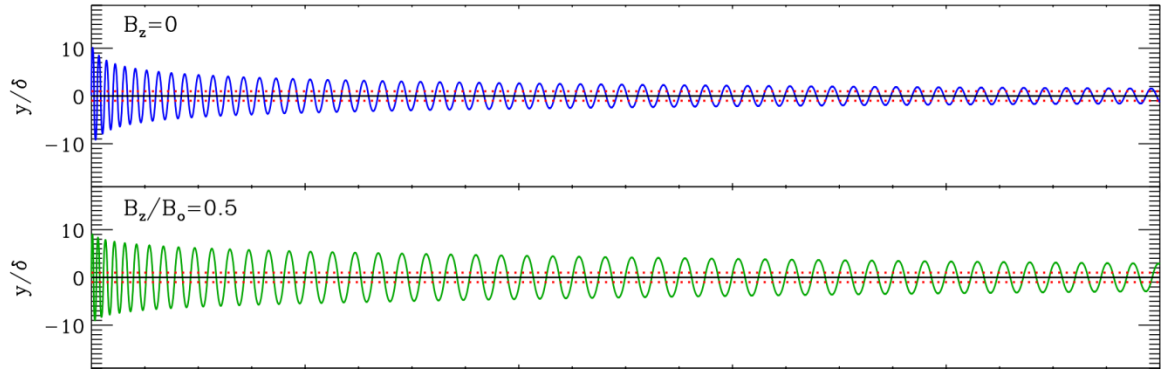

Contopoulos 2007; Cerutti et al. 2012, 2015

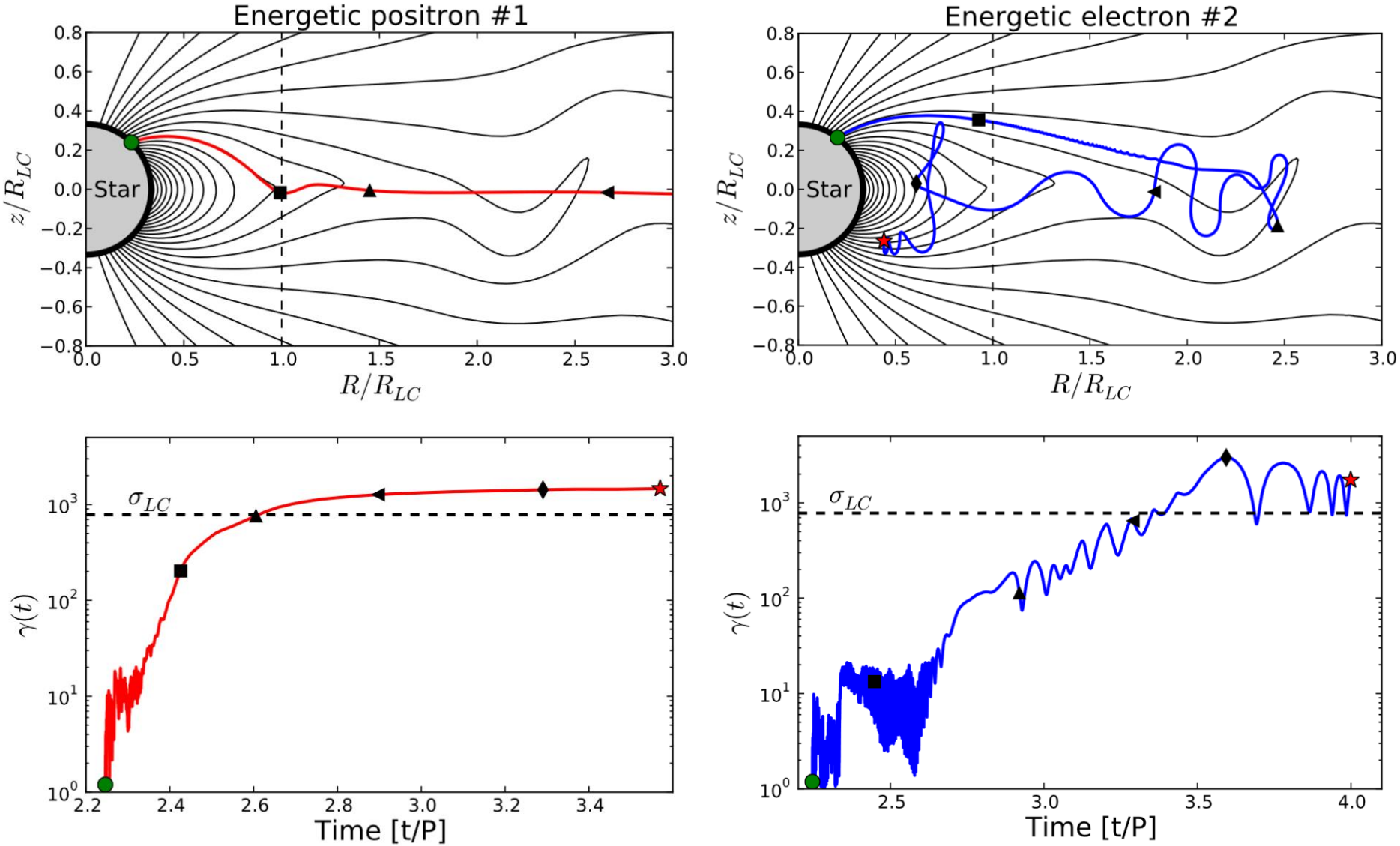

Cerutti et al. 2015

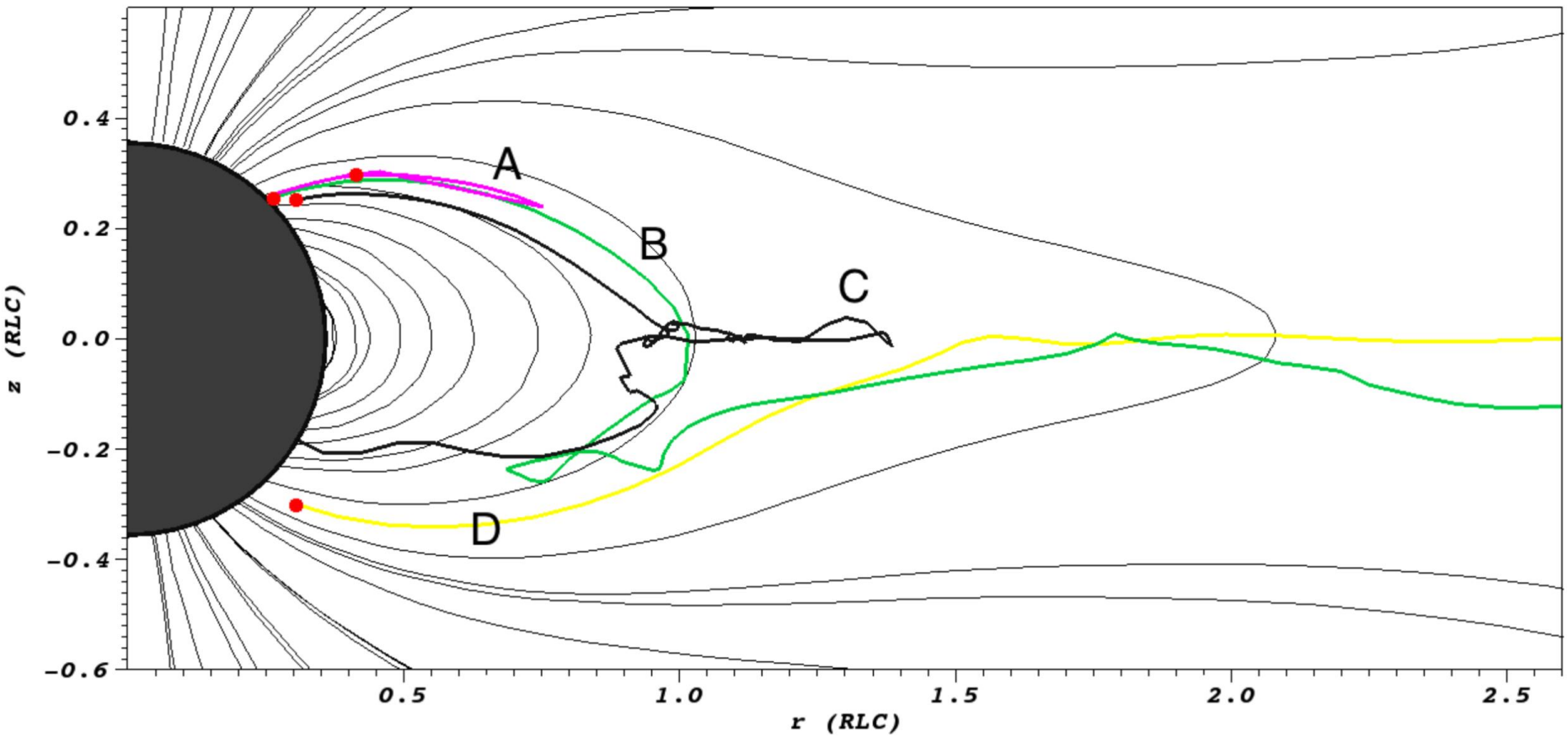

Brambilla, Kalapotharakos et al. 2018

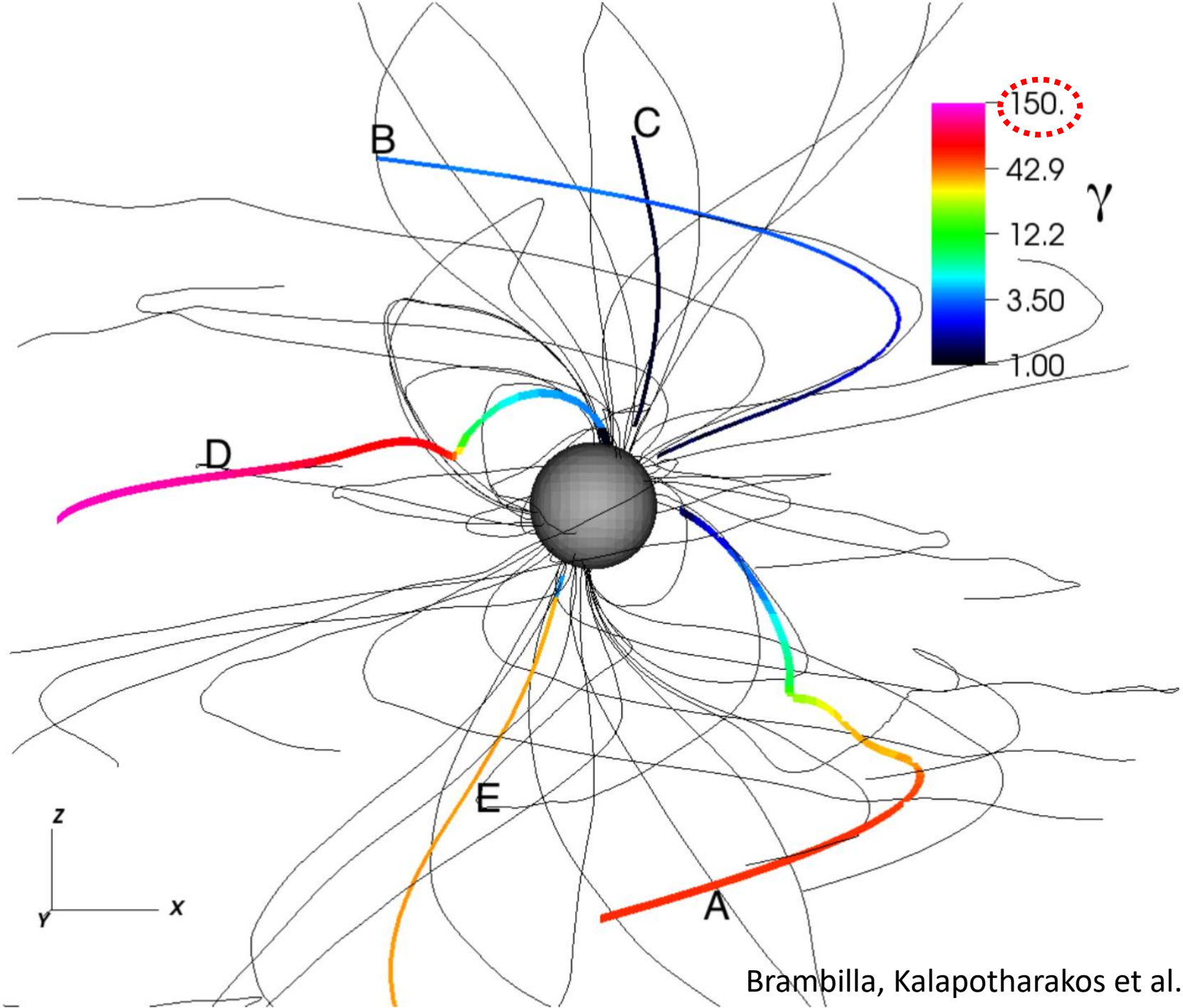

Brambilla, Kalapotharakos et al. 2018

The key is current closure!

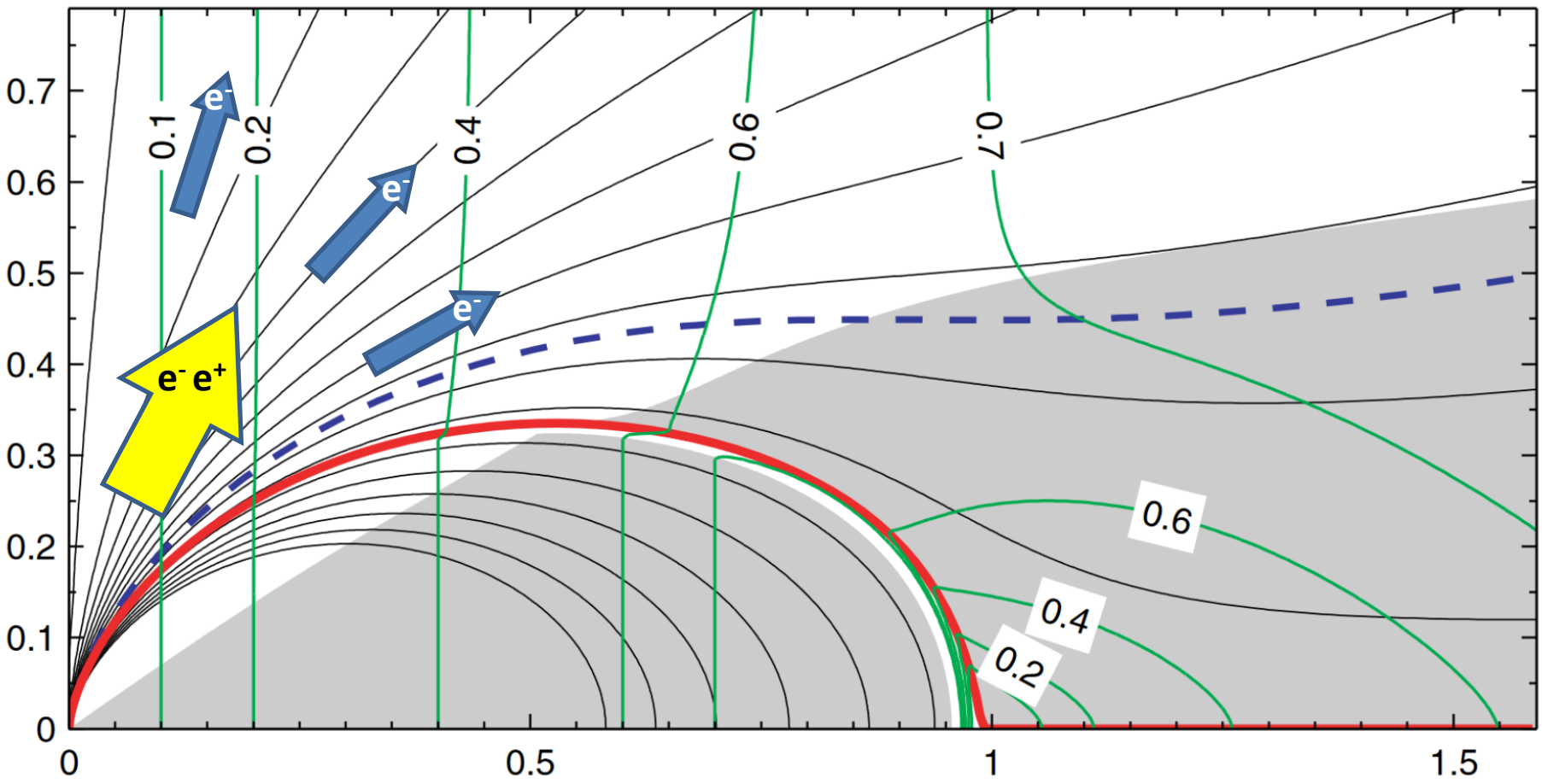

Timokhin 2006

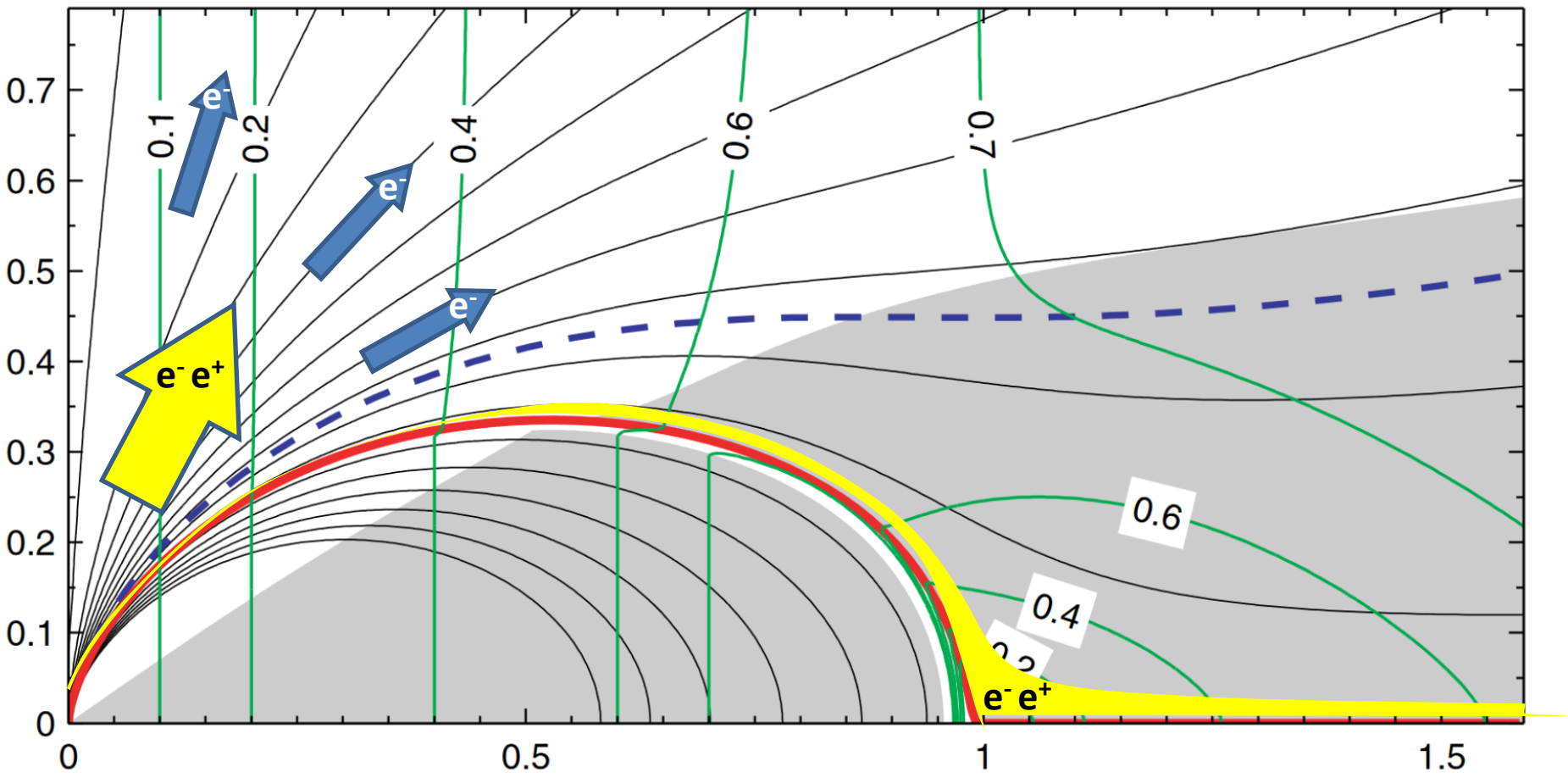

Timokhin 2006

Contopoulos 2019; Contopoulos & Stefanou 2019; Contopoulos, Petri & Stefanou 2019

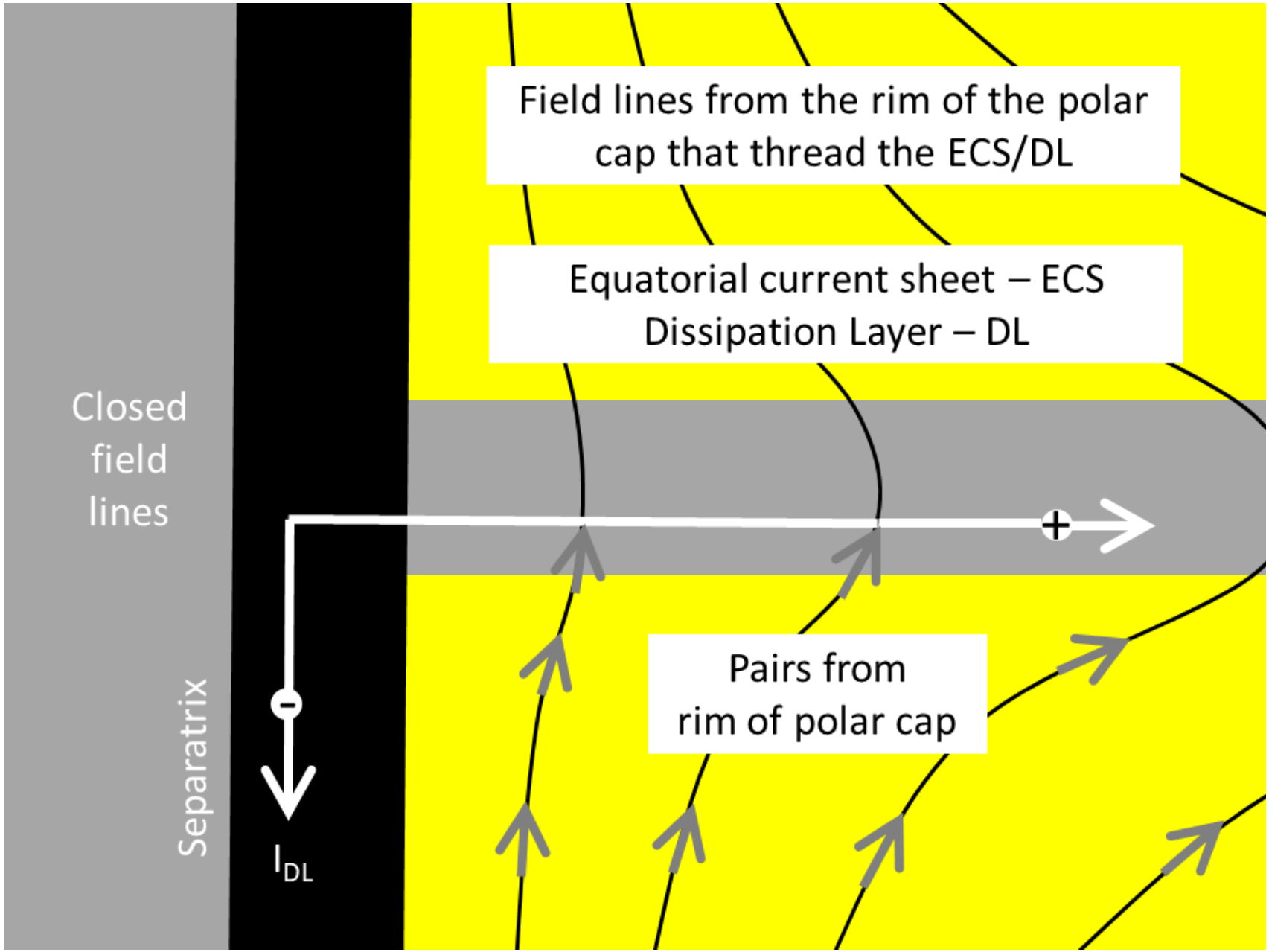

Contopoulos 2019; Contopoulos & Stefanou 2019; Contopoulos, Petri & Stefanou 2019

Current closure in the pulsar magnetosphere

I. Contopoulos[1,2]★

a flux of electron-positron pairs equal to $2\pi r_{\rm pc}\delta\kappa\rho_{\rm GJ}c/e$. The electron content in that narrow region is sufficient to support the return current $I_{\rm separatrix}$ in the separatrix, provided that

$$\delta \approx \frac{I_{\rm separatrix}}{\kappa r_{\rm pc}\Omega B_*} \ . \tag{7}$$

The natural way for these pairs to supply the electrons needed to form the separatrix return current is the *development of a dissipation zone just outside the Y-point at the origin of the equatorial current sheet on the light cylinder* (see description in Figure 1). In that

MNRAS **000**, 000–000 (0000) Preprint 12 October 2018 Compiled using MNRAS LaTeX style file v3.0

Current closure in the pulsar magnetosphere

I. Contopoulos[1,2]★

$$L_\gamma \approx \frac{\delta}{r_{\rm pc}} \dot{E} = \frac{\dot{E}}{2\kappa} \, . \tag{10}$$

This simple relation tells us that for typical γ-ray pulsars with observed γ-ray luminosity efficiencies equal to $0.1\% - 1\% - 10\%$, the corresponding pair formation multiplicities are expected to lie in the range $\kappa \approx 500 - 50 - 5$ respectively. Notice also that, if we assume that $L_\gamma/\dot{E}$ is roughly proportional to $\dot{E}^{-1/2}$ as suggested by observations (Thompson 2008; Grenier & Harding 2015), then $\kappa \propto \dot{E}^{1/2}$.

MNRAS **000**, 000–000 (0000) Preprint 12 October 2018 Compiled using MNRAS LaTeX style file v3.0

Current closure in the pulsar magnetosphere

I. Contopoulos[1,2]★

$$\Delta \approx 2\delta \left(\frac{r_{\rm lc}}{r_*}\right)^{3/2} \approx \frac{r_{\rm lc}}{\kappa} \,, \tag{15}$$

and hence, the accelerating electric field in that region is equal to

$$E_{\rm acc} \approx \frac{V_{\rm rim}}{\Delta} \approx B_{\rm lc} \,. \tag{16}$$

The "ring of fire"

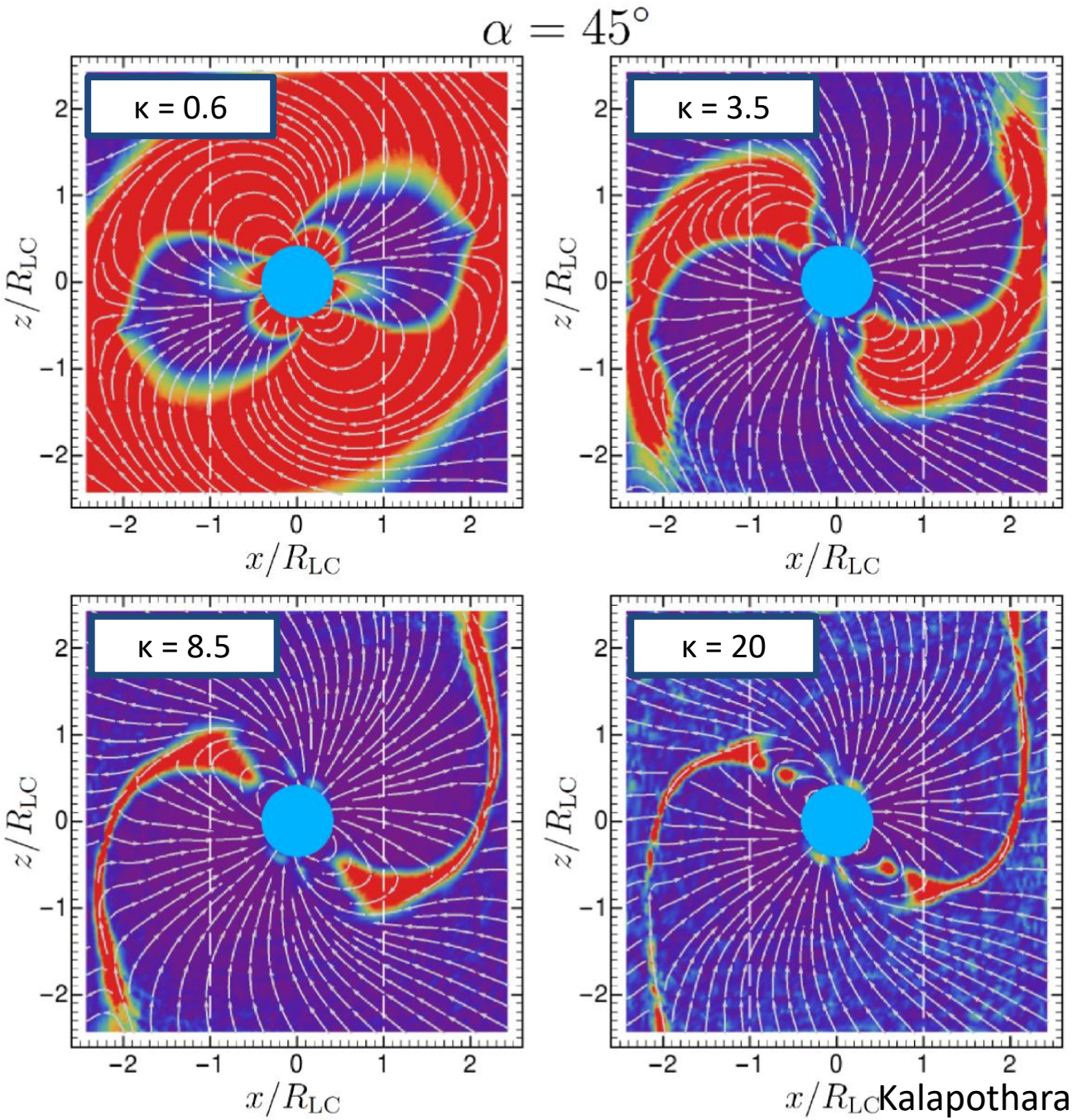

Kalapotharakos et al. 2018

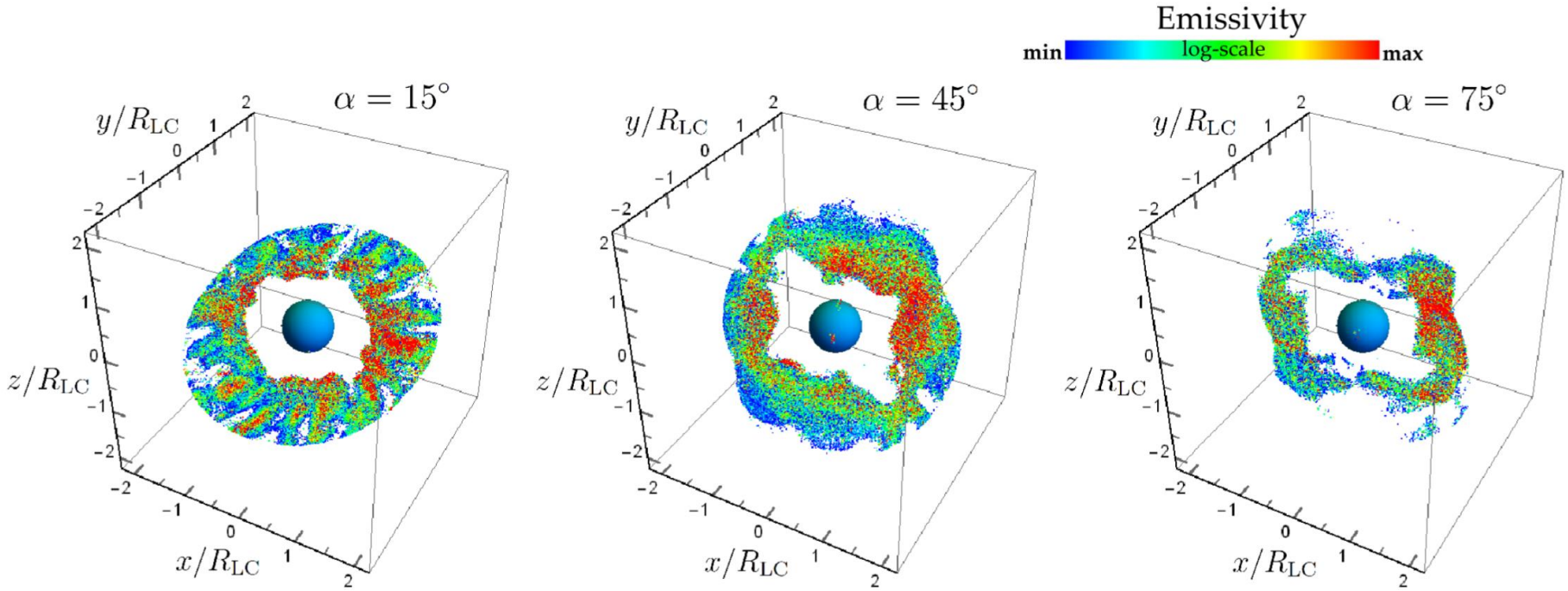

κ = 28

Kalapotharakos et al. 2018

Hybrid calculations:
FFE everywhere + dissipative ECS
(particle acceleration with radiation reaction)

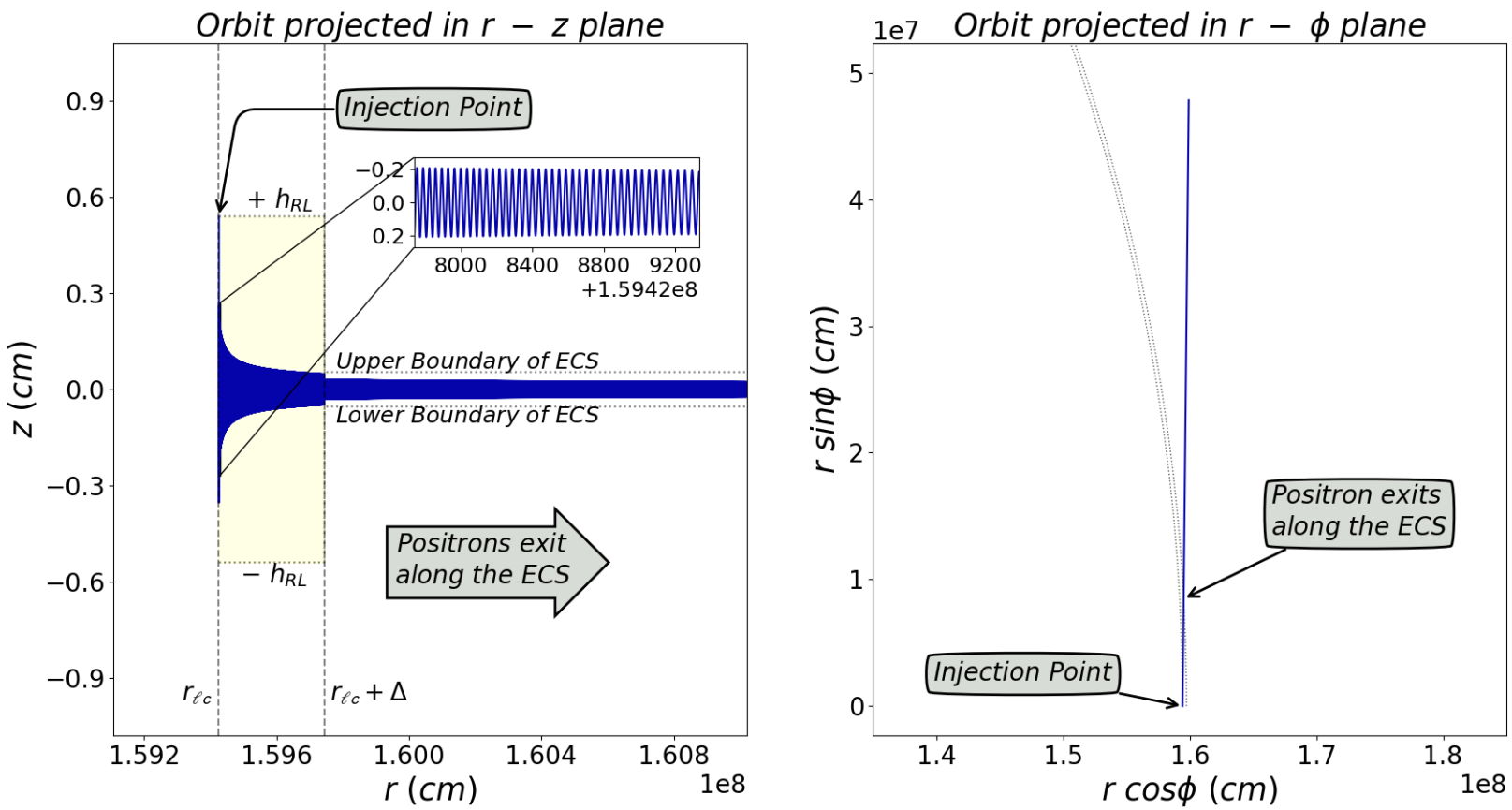

"A ring-of-fire in the pulsar magnetosphere", Contopoulos & Stefanou 2019

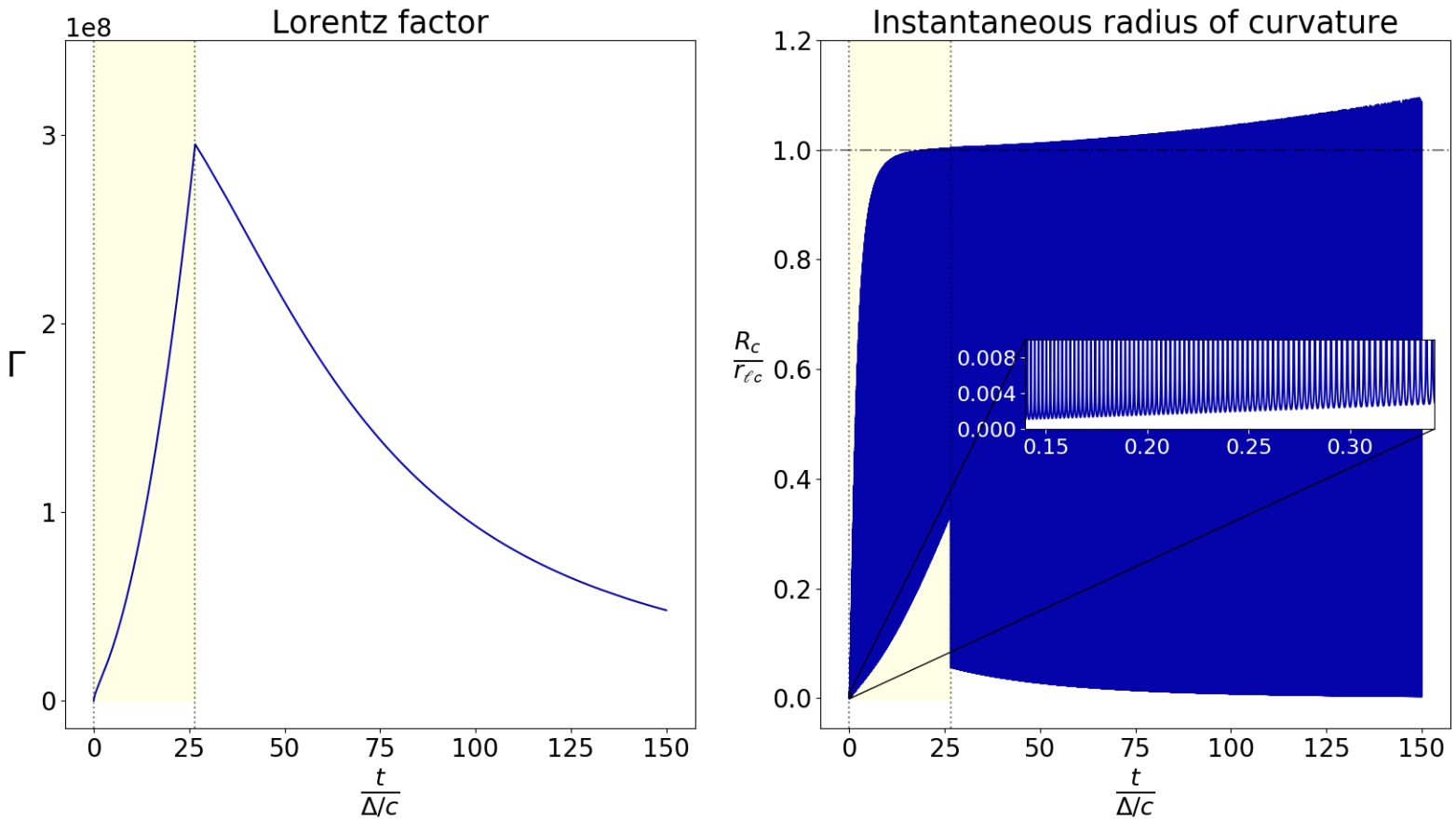

"A ring-of-fire in the pulsar magnetosphere", Contopoulos & Stefanou 2019

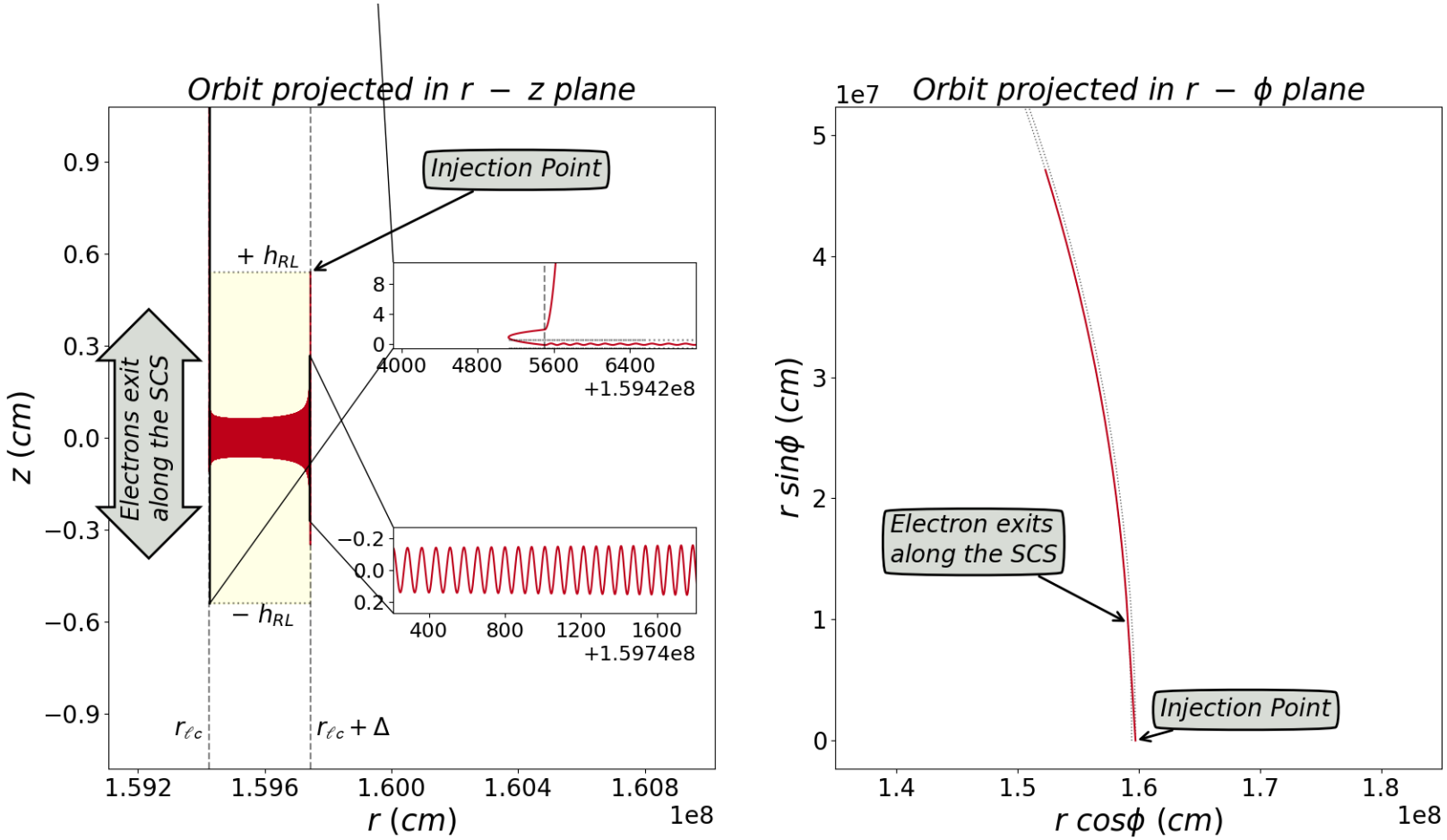

"A ring-of-fire in the pulsar magnetosphere", Contopoulos & Stefanou 2019

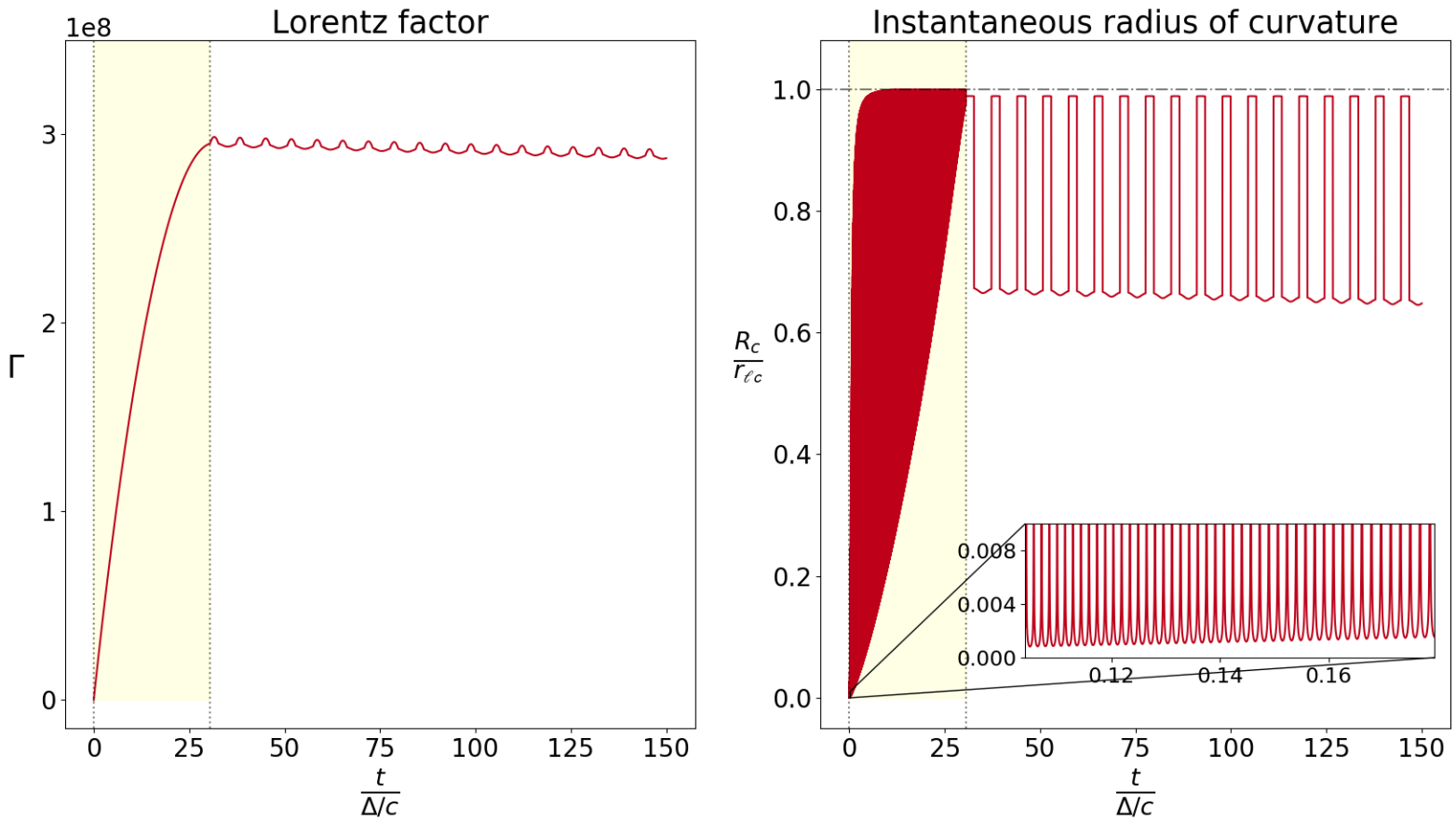

"A ring-of-fire in the pulsar magnetosphere", Contopoulos & Stefanou 2019

MNRAS **000**, 000–000 (0000) Preprint 12 October 2018 Compiled using MNRAS LaTeX style file v3.0

Current closure in the pulsar magnetosphere

I. Contopoulos[1,2]★

calculate the asymptotic particle Lorentz factor Γ in the curvature radiation reaction limit,

$$\frac{d\Gamma}{dt} = \frac{ecE_{acc}}{m_e c^2} - \frac{2e^2\Gamma^4}{3r_{lc}^2 m_e c} = 0 \Rightarrow \Gamma_{rrl} = \left(\frac{3r_{lc}^2 E_{acc}}{2e}\right)^{1/4} . \quad (14)$$

Here, E_{acc} is the accelerating electric field in the dissipation region. We have assumed here that the radius of curvature around the Y-point is equal to r_{lc}. We can estimate E_{acc} if we make the simplifying assumption that the magnetic flux that crosses the equatorial dissipation zone does so in a dipole-like configuration. In that case, the width Δ of that region is equal to

$$\Delta \approx 2\delta\left(\frac{r_{lc}}{r_*}\right)^{3/2} \approx \frac{r_{lc}}{\kappa} , \quad (15)$$

and hence, the accelerating electric field in that region is equal to

$$E_{acc} \approx \frac{V_{rim}}{\Delta} \approx B_{lc} . \quad (16)$$

We have thus shown that the accelerating electric field is approximately equal to the value of the magnetic field near the light cylinder. One can easily check that, with this accelerating electric field,

$$\Gamma_{rrl} = 4\times 10^7 \left(\frac{B_*}{10^{13}\mathrm{G}}\right)^{1/4}\left(\frac{P}{1\ \mathrm{s}}\right)^{-1/4} , \quad (17)$$

where, P is the pulsar period. This will be reached within an acceleration distance on the order of

$$l_{acc} \equiv \frac{\Gamma_{rrl}\, m_e c^2}{eE_{acc}} \approx 0.4\left(\frac{B_*}{10^{13}\ \mathrm{G}}\right)^{-3/4}\left(\frac{P}{1\ \mathrm{s}}\right)^{7/4} r_{lc} . \quad (18)$$

Obviously, the acceleration in the equatorial dissipation region will be able to reach the radiation reaction limit only if $l_{acc} \le \Delta$, i.e. if $P \lesssim \kappa^{-4/7}$ s. This will be satisfied only for young pulsars. For slower pulsars, the radiation reaction limit is probably not reached in the equatorial dissipation region. In that case, the particles that will benefit from the full potential drop accross the rim region will be accelerated to a maximum Lorentz factor Γ_{max} equal to

$$\Gamma_{max} = \frac{eE_{acc}\Delta}{m_e c^2} = \frac{eB_* r_*^3}{2\kappa r_{lc}^2 m_e c^2} = \frac{10^8}{\kappa}\left(\frac{B_*}{10^{13}\ \mathrm{G}}\right)\left(\frac{P}{1\ \mathrm{s}}\right)^{-2} . \quad (19)$$

The curvature radiation γ-ray cutoff energy will thus be determined by the smallest of Γ_{max} and Γ_{rrl}, namely

$$\epsilon_{cut} = \min(\Gamma_{max}^3, \Gamma_{rrl}^3)\,\frac{3hc}{2r_{lc}}$$

$$= \frac{80}{\kappa^3}\left(\frac{B_*}{10^{13}\ \mathrm{G}}\right)^3\left(\frac{P}{1\ \mathrm{s}}\right)^{-7}\ \mathrm{GeV} \quad \text{if } \Gamma_{max} < \Gamma_{rrl} , \quad (20)$$

$$3\left(\frac{B_*}{10^{13}\ \mathrm{G}}\right)^{\frac{3}{4}}\left(\frac{P}{1\ \mathrm{s}}\right)^{-\frac{7}{4}}\ \mathrm{GeV} \quad \text{if } \Gamma_{max} > \Gamma_{rrl} . \quad (21)$$

Hybrid simulations:
FFE everywhere + dissipative ECS
(self-consistent particle orbit calculation)

Summary

- Ab initio PIC simulations give us important hints:
  - Ideal Force-Free everywhere except in
  - Dissipative Equatorial Current Sheet
- Hybrid simulations:
  - Self-consistent calculation
  - FFE everywhere
  - Realistic particle trajectories only in the ECS
- High-energy radiation from the particles accelerated in the ECS

PHAROS

THE MULTI-MESSENGER PHYSICS AND ASTROPHYSICS OF NEUTRON STARS

COST Action PHAROS Annual Conference: Greece 2020